Application of lipocalin-type prostaglandin D synthase (L-PGDS) as a novel solubilizer for solid oral dosage forms

Application of lipocalin-type prostaglandin D synthase (L-PGDS) as a novel solubilizer for solid oral dosage forms

（リポカリン型プロスタグランジン D 合成酵素の
経口固形製剤開発における新規可溶化剤としての応用）

Masashi Mizoguchi

Osaka Prefecture University
Osaka, Japan
March 2016

Contents

List of Abbreviations

API:	active pharmaceutical ingredient
AUC:	area under the serum or plasma concentration-time curve
BCS:	biopharmaceutics classification system
cAMP:	cyclic adenosine monophosphate
CD:	circular dichroism
cGMP:	cyclic guanine monophosphate
C_{max}:	maximum concentration
DMSO:	dimethyl sulfoxide
DVS:	dynamic vapor sorption
EPR:	enhanced permeability and retention
FaSSGF:	fasted state-simulated gastric fluid
FaSSIF:	fasted state simulated intestinal fluid
L-PGDS:	lipocalin-type prostaglandin D synthase
HPLC:	high-performance liquid chromatography
PBS:	phosphate buffer solution
PLGA:	poly (lactic-co-glycolic acid)
RH:	relative humidity
SBP:	systolic blood pressure
SDS:	sodium dodecyl sulfate
SDS-PAGE:	sodium dodecyl sulfate polyacrylamide gel electrophoresis
SE-HPLC:	size exclusion high-performance liquid chromatography
SEM:	scanning electron microscope
SGF:	simulated gastric fluid
SHR:	spontaneously hypertensive rats
SMEDDS:	self-microemulsifying drug delivery system
T_{max}:	time to maximum concentration
$T_{1/2}$:	elimination half-life

1
Introduction and objectives of the thesis

1.1 Introduction

According to the recent approach shift for drug discovery from the phenotypic to target-based approach, only the efficacy of candidate is focused and the candidate proceeding to the next development phase is selected in the discussion without any information on the physicochemical properties, such as solubility, polymorphism, etc. In addition, the chemical structure of candidate has become complicated by the technological evolution of chemical synthesis and many newly synthesized compounds have the undesirable physicochemical properties, such as poor solubility, high lipophilicity, and high molecular weight [1, 2]. Although the solubility of drug compound is known to be one of the limiting factors for oral bioavailability, the number of drug candidates that shows insoluble or poorly-soluble characteristics in water has been increasing markedly in the development stage of the pharmaceutical industry. The result of publication search in Scopus (https://www.scopus.com/) indicated an increased number of publications on “poorly-water soluble drug”, and its characteristics and counter measures further denoted that studies related to this topic has become one of the academic curiosities (Fig. 1). In addition, the categorization for the launched drug product in USA and new chemical entities developed in the pharmaceutical company based on Biopharmaceutics Classification System (BCS), which categorize the solid oral drug product into four classes based on the solubility and permeability of the compounds [3], has reported that the percentage of BCS class II and IV which show low solubility has increased markedly [4] (Fig. 2). On the other hand, the verification

of proof of concept is required as early as possible in the early stage of drug development. The current mainstream for development strategy has shortened the time frame to develop the appropriate formulation for the poorly water-soluble candidate. Hence, poor solubility has become an industry-wide concern.

Several approaches have been investigated and developed to overcome the concerned solubility issue of candidates [5, 6]. One of the viable approaches is the structural modification of compounds, such as pro-drug, salt formation, and co-crystal. This approach improves the solubility of target poor water soluble compounds by simple chemical modification of drug molecules. However, the pro-drug approach has the possibility to reduce the pharmacological efficacy caused by the chemical modification, and the polymorph control with marked efforts for salt and co-crystal formation is needed.

Another approach of modification is the physical modification of compound that includes particle size reduction, solid dispersion, amorphization, pH modification, lipid based systems, and so on. This approach aims at the enhancement of solubility of poorly-water soluble compounds by the combination of excipient and designated manufacturing process. However, the optimization for the amount of excipient and process parameter is a meticulous challenge for the formulation scientists. Furthermore, the usage of excipients for the approach is commonly limited due to the safety concerns. It has been reported that cyclodextrin may reduce drug absorption as opposed to solubility enhancement as a result of the decrease in the drug's free fraction available for absorption [7-9]. In addition, the potential instability of active pharmaceutical ingredient (API) is a common outcome for both the approaches [10, 11]. The current available technologies need the careful verification on many factors to obtain the solubility improvement of the target compounds.

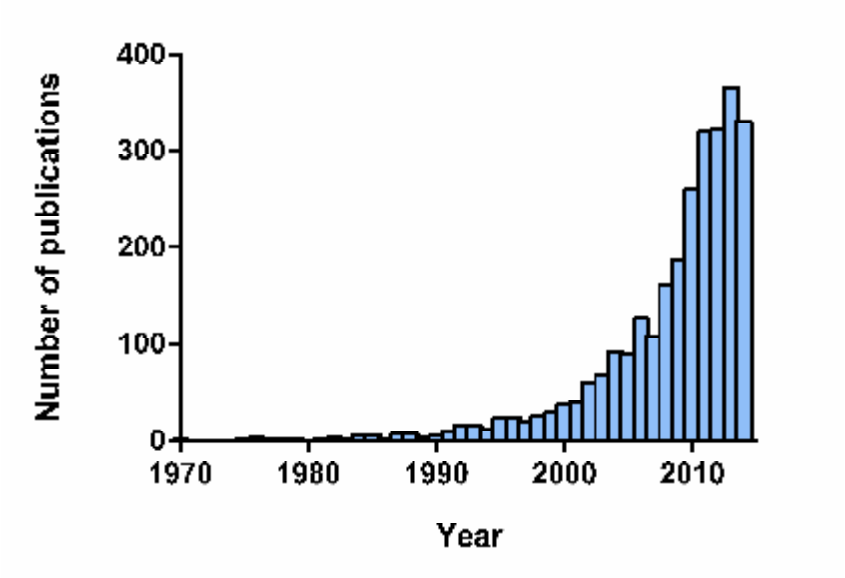

Figure 1 Number of publications including term “poorly-water soluble drugs” in Scopus

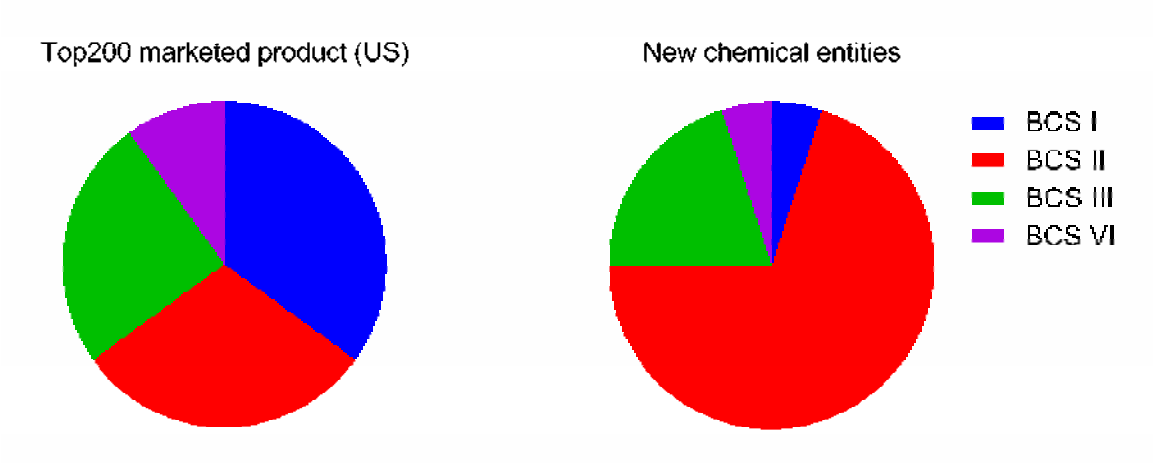

Figure 2 BCS distribution for Wyeth NCEs and marketed products [4].

1.1.1 Lipocalin-type prostaglandin D synthase (L-PGDS)

L-PGDS (Fig, 3) is a multi-functional protein that plays the role of a catalyzer in the isomerization of prostaglandin H_2, a scavenger for reactive oxygen species, and an extracellular transporter for small lipophilic molecules as a member of the lipocalin superfamily [12-14]. Recently, it was demonstrated that L-PGDS acted as a scavenger of biliverdin, a metabolite of hemoglobin that accumulates in the cerebrospinal fluid

of patients with aneurysmal subarachnoid hemorrhage [15].

The structure of L-PGDS exhibits the typical lipocalin fold, consisting of an eight-stranded, antiparallel β-barrel and a long α-helix associated with the outer surface of the barrel. The interior of the barrel forms a hydrophobic cavity opening into the upper end of the barrel, the size of which is larger than those of other lipocalins [16-18]. Based on the structure of L-PGDS, it has been demonstrated that L-PGDS could bind to a large variety of lipophilic molecules, such as heme metabolites, retinoids, thyroids, steroids, flavonoids, and saturated fatty acids in the hydrophobic cavity [19, 20]. The mechanism for complex formation between L-PGDS and the guest compounds consisted of both hydrophilic and hydrophobic interactions adjusted by enthalpy-entropy compensation [21].

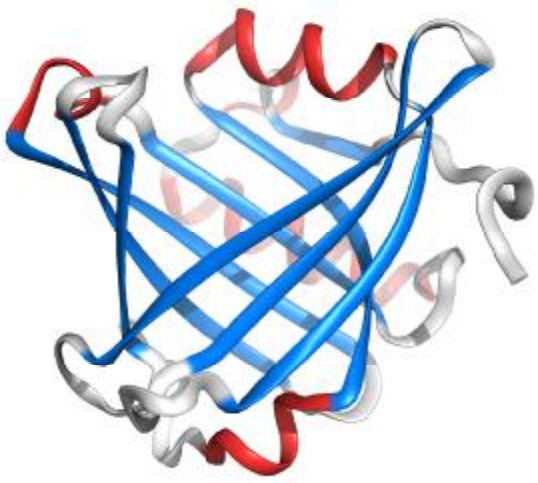

Figure 3 Three-dimensional structure of human L-PGDS (molecular mass: 18777.7, PDB code: 3O2Y).

1.1.2 Drug delivery system using L-PGDS

The feasibility of L-PGDS as a novel drug-delivery carrier to improve the solubility of the poorly water-soluble molecules has already been evaluated as one of its major functionality as per the previous study [22]. In addition, the following profiles are

considered in the development of L-PGDS as drug delivery carrier. A previous study reported L-PGDS to be highly biocompatible due to its bimolecular nature and was also demonstrated with low immunogenicity.[22]

According to the mechanism of complexation with the guest compounds, the initial drug burst and drug leakage was potentially concerned like poly (lactic-co-glycolic acid) (PLGA) nanoparticles [23, 24]. The targeting ability was unknown, but the passive targeting by the enhanced permeability and retention (EPR) effect was considered due to the carrier size. The targeting improvement was expected by the design of fusion protein and pegylation like albumin [25]. Although the solubilizing capacity of L-PGDS may be limited by the size of guest compounds to that of L-PGDS cavity size, the capability for the current development of low-molecular-weight drug candidates could be sufficient. Indeed, L-PGDS can bind and solubilize the hydrophobic guest compounds approximately up to M_w= 850. These profiles, taken together, the potential application of L-PGDS for the drug delivery carrier is considered to show the passive targeting ability and improvement of drug absorption as a solubilizer. The profile of L-PGDS from the aspect of drug delivery carrier is summarized and compared with the other drug delivery carriers presented in Table 1.

Table 1 Summary for the application of L-PGDS as drug delivery carrier and the comparison with the developed technologies [23-36]

	L-PGDS	Nanoparticle	Liposome	Immuno-conjugate	Cyclodextrin	Albumin
Safety	- Good biodegradability and biocompatibility - Low immunogenicity - Potential API burst	- Good biodegradability and biocompatibility - Low immunogenicity - Potential API burst	- Good biodegradability and biocompatibility - Low immunogenicity - Potential API burst	- Good biodegradability and biocompatibility - Low immunogenicity - Concerned stability of linker	- Good biodegradability and biocompatibility - Low immunogenicity - Potential API burst	- Good biodegradability and biocompatibility - Low immunogenicity
Stability	Unclear	Stable	Stable	Stable	Stable	Stable
Manufacturability	- Complex process - High cost	- Complex process - High cost	- Complex process - High cost	- Complex process - High cost	- Simple process - Low cost	- Complex process - High cost
Flexibility	Not investigated	Surface modification (e.g. Pegylation)	Surface modification (e.g. Pegylation)	Type of antibody	Three basic structure and multiple chemical modification	Polymerization (Linker binding, Fusion protein)
Tumor-targeting	- EPR effect	- EPR effect - Immunotargeting	- EPR effect - Immunotargeting	- EPR effect - Immunotargeting	- EPR effect	- EPR effect
Guest molecule	- Low molecular weight compounds	- Low molecular weight compounds - Protein/peptide - Nucleic acid	- Low molecular weight compounds - Protein/peptide - Nucleic acid	- Low molecular weight compounds	- Low molecular weight compounds	- Low molecular weight compounds - Protein/peptide - Nucleic acid
Inclusion efficiency	High (dependent on guest molecule)	Low	Low	Low	High (dependent on guest molecule)	Low
Dosage form	- Intravenous - Oral - Pulmonary	- Intravenous	- Intravenous - Oral	- Intravenous	- Intravenous - Oral - Eye drop	- Intravenous

L-PGDS, lipocalin-type prostaglandin D synthase; API, active pharmaceutical ingredient; EPR, enhanced permeability and retention

1.1.3 Stability of protein formulations

Based on the manufacturing process, the recombinant protein is produced in solution state after several isolation and purification processes. However, proteins in liquid formulation are generally at a greater risk of chemical and physical instability [37]. In addition, the basic shelf-life of liquid state protein formulation is considered as shorter for the conventional usage as the pharmaceutical excipient, and several factors, such as storage condition and sterilization need to be controlled carefully for the storage of protein solution [38-40]. Therefore, the proteins need to be prepared in dry form in order to increase the stability and its application as multiple dosage forms (Table 2).

Table 2 Characteristic comparison in the different state of protein products

Characteristic	**Solution**	**Dried powder**
Storage condition	5°C	Possibly room temperature or less
Typical shelf-life	1 month	2-3 years
Requirement of sterile conditions or Addition of antibacterial agent	Yes	No
Applicability for multiple dosage forms as conventional excipients	Low (Injection, capsule)	High (Tablet, capsule, inhaler, injection, etc.)

1.1.4 Drying technology for proteins

1.1.4.1 Lyophilization

Lyophilization process consists of two major processes, freezing of protein solution and drying of the frozen solid under vacuum. In addition, the drying step is further divided into two phases: primary and secondary drying [37] (Fig. 4). The primary drying removes the frozen water and the secondary drying removes the non-frozen 'bound' water. Lyophilization is a simple process that exhibits least thermal influence on the protein. However, the lyophilization process is considered to be energy-intensive, and its freezing or drying processes may have the potential influence to destabilize or unfold/denature the target protein. Furthermore, the process involves time-consuming steps, such as freezing, followed by drying under low pressure, with involvement of high production costs [38]. In addition, the lyophilized particles are coarse and the size reduction of the produced particles needs to be applied to the usage for multiple dosage forms, such as tablets and inhalation formulation.

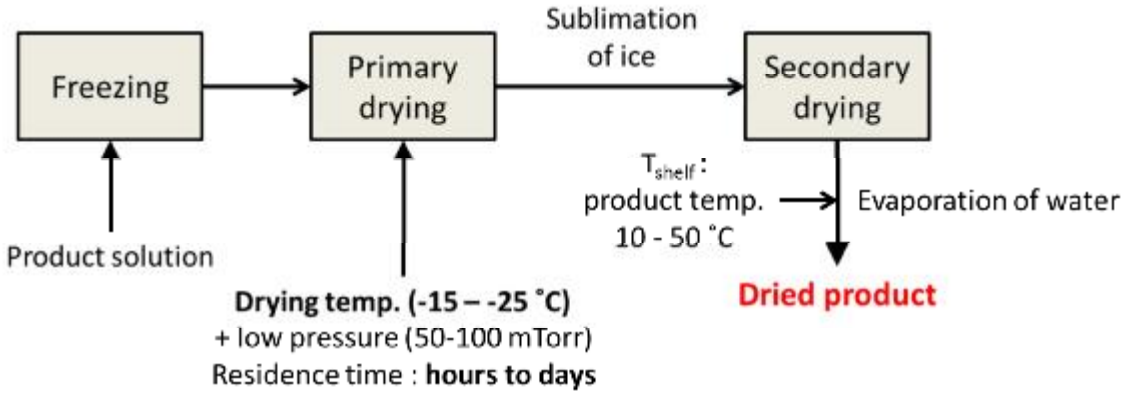

Figure 4 Unit operations involved in lyophilization [37]

1.1.4.2 Spray drying

The spray-drying process utilizes heat to evaporate micro-dispersed droplets created by atomization of a continuous liquid feed. The process involves three steps of operation: atomization, dehydration, and powder collection. As shown in Fig. 5, the protein solution feed is sprayed by an atomizer into a drying chamber. Aided by the large specific surface area of the droplets and hot air, dehydration takes place in seconds in the laboratory-scale drying chamber. The one-step drying process leads to a significantly shorter operation time and cost-effective dehydration [41]. In addition, the spray-dried powder commonly shows spherical fine powder, and the obtained powder from spray drying process is considered to be suitable for the multiple dosage forms. However, the various stresses during spray drying, such as shearing stress, liquid/air interfacial expansion, and heat transfer may affect the stability and aggregation of protein [42].

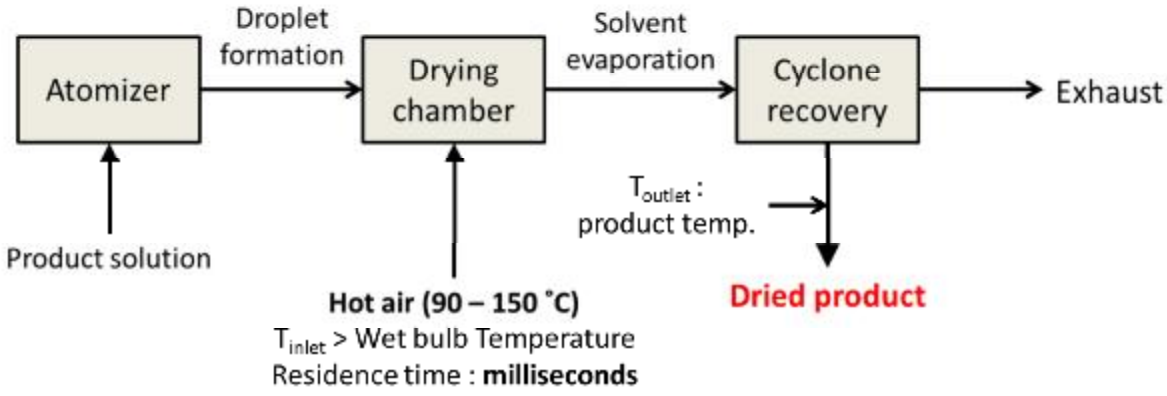

Figure 5 Unit operations involved in spray drying [37]

1.2 Objectives of thesis

The present study focuses on the one of the L-PGDS functions that deals with improving the solubility of poorly-water soluble compounds by forming complex. The study aims at evaluation of the feasibility of L-PGDS as the pharmaceutically functional excipient.

The specific objectives of the present study are as follows:

- To develop the preparation method of spray-dried drug substance/L-PGDS complex.
- To evaluate of the physicochemical characteristics of the prepared particles.
- To evaluate *in vivo* utility of drug substance/L-PGDS complex.
- To assess the potential stability profile of spray-dried drug substance/L-PGDS complex.

Telmisartan has been used as the model compound in Chapter 2, and the development of the preparation method for telmisartan/L-PGDS complex, and the optimization of process parameters for the spray drying process for complex solution has been described. In addition, physicochemical characteristics, the *in vitro* and *in vivo* performance of the developed formulation are evaluated in Chapter 2.

Chapter 3 describes the development of pH-independent drug release formulation for basic compound using L-PGDS. Dipyridamole has been used as the model basic compound that shows pH-dependent solubility profile.

Finally, chapter 4 describes the potential stability profile of spray-dried dipyridamole/L-PGDS complex formulation.

2

Investigation of L-PGDS as a novel solubilizer for poorly soluble compounds

2.1. Introduction

Telmisartan (Fig. 6) is an antagonist of the angiotensin II type-1 receptor that is indicated for the treatment of hypertension [43]. Telmisartan is categorized as a BCS class II compound, and its solubility is quite low within the physiological gastrointestinal pH range [44]. According to the chemical structure of telmisartan, the compound is readily ionizable with pH-dependent solubility (Fig. 6 and Fig. 7).

The inherent solubility profile applies to the solubilization, and the microenvironmental pH modification has been investigated as the solubilization approach [45]. Although the solubilization approach with pH modification is an effective method, this method can be applied to ionizable API as a prerequisite. In addition, the formulation including pH modifier has a high risk of chemical instability and poor manufacturability caused by the acidifier or alkalizer [46, 47]. Therefore, careful qualitative and quantitative selections of pH modifiers are required. Furthermore, the solubility improvement by the formation of a solid dispersion using a pH modifier incorporating a common pharmaceutical solubilizer, such as an organic solvent, cyclodextrin, and surfactant has also been demonstrated.

However, a series of solubilizing approaches requires the combination of several solbilizers to achieve adequate solubility of telmisartan. The marketed formulations of telmisartan are mainly formulated with solid dispersion technique using proportionally

high concentration of strong alkalizer, such as sodium hydroxide and meglumine or combinations thereof [48-50].

In this chapter, I showed the application of L-PGDS as a novel drug-solubilizing carrier for an oral solid formulation using telmisartan as a model compound. The solid state of the telmisartan and L-PGDS complex formulation was produced using the spray-drying technique, and the physicochemical properties of the produced particles were further characterized. Finally, the *in vitro* and *in vivo* performance of the developed formulation was assessed.

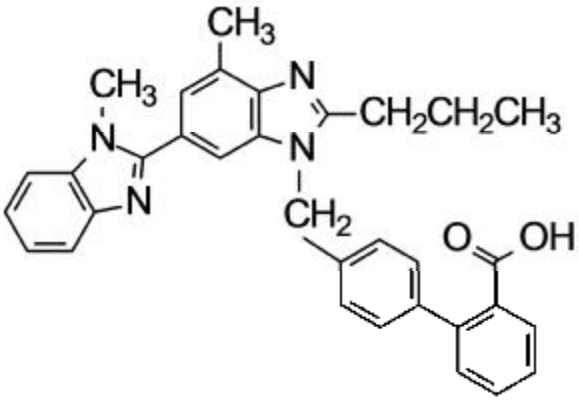

Figure 6 Chemical structure of telmisartan [relative molecular mass: 514.6].

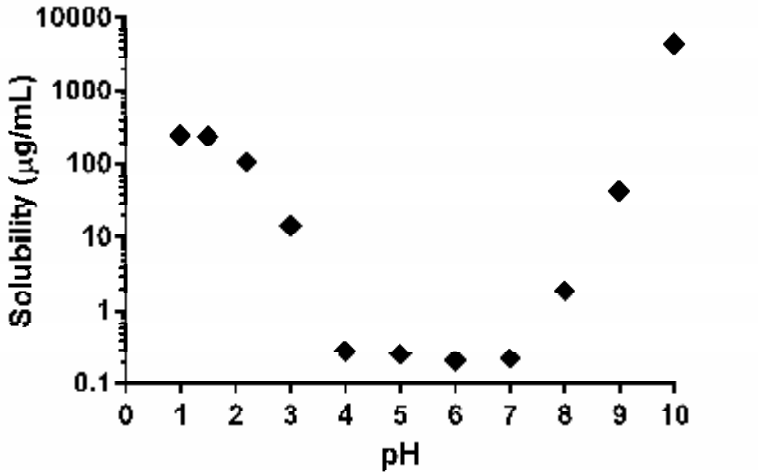

Figure 7 pH-solubility profile of telmisartan

2.2. Materials and methods

2.2.1. Materials

Telmisartan and the commercial products (Micardis®) were supplied by Boehringer Ingelheim GmbH & Co. KG (Ingelheim, Germany). Jet-milling of telmisartan was carried out by A-O jet mill (Seishin Enterprise Co., Ltd, Osaka, Japan). The injector and grinding air pressures were 7.5 bar, and powder feed rate was set to 3 g/min at room temperature. All other chemicals were of analytical grade.

2.2.2. Purification of recombinant human L-PGDS

In the present study, in case of the recombinant human C65A/C167A (ε_{280} =25,900 M^{-1} cm^{-1})-substituted L-PGDS mutant, a catalytic residue of cysteine was substituted to alanine to get rid of an enzymatic activity of L-PGDS. The 22 N-terminal amino acid residues corresponding to the putative secretion signal peptide of L-PGDS were truncated. C65A/C167A-substituted L-PGDS was expressed in *Escherichia coli* BL21 (DE3) (TOYOBO, Osaka, Japan) [20]. The site-directed mutagenesis was performed using the QuikChange™ site-directed mutagenesis kit (Stratagene California, La Jolla, California, USA). The mutated L-PGDS was expressed as a glutathione S-transferase fusion protein. The fusion protein was bound to a glutathione–Sepharose 4B column (GE Healthcare Bio-Sciences) and incubated overnight with thrombin (16.5 units/mL column bed volume) to release L-PGDS at room temperature. The protein was further purified by gel filtration chromatography with HiLoad 26/600 Superdex 75 (GE Healthcare Bio-Sciences) in 5 mM Tris-HCl (pH 8.0). The purified L-PGDS of 100-200 mg was rou-

tinely obtained from 1L of culture.

2.2.3. Solubility study

An excess amount of telmisartan was weighed in a 2 mL microtube with 1 mL of aqueous solution containing several kinds of buffer medium in the presence of L-PGDS or without L-PGDS. The sealed microtubes were shaken with a Rotator RT-50 (TAITEC, Saitama, Japan) at 37°C, followed by filtration through a 0.45 μm filter (EMD Millipore, Billerica, Massachusetts, USA). After incubation, the sample solution was diluted with methanol and centrifuged at 3,000 rpm for 10 min. Then, 20 μL of filtered supernatant (0.45 μm filter) was injected into a high-performance liquid chromatography (HPLC, Waters Corporation, Milford, Massachusetts, USA) equipped with a YMC Pack ODS-AM column (150 x 4.6 mm I.D., 5 μm, YMC Co., Ltd., Kyoto, Japan) to analyze the amount of telmisartan. The mobile phase consisted of a mixture of methanol and 2% (w/v) ammonium phosphate (pH 3.0) (70:30, v/v), and was eluted at a flow rate of 1 mL/min. The chromatogram was monitored at 297 nm.

2.2.4. Spray drying of telmisartan/L-PGDS complex solution

Based on the solubility study, the complex of L-PGDS and telmisartan was prepared in the molar ratio of 1:1. The complex solution was filtered with a 0.45 μm filter (EMD Millipore) before the spray-drying process. The dried L-PGDS or telmisartan/L-PGDS complex was prepared with Mini Spray Dryer B-290 (BÜCHI Labortechnik AG, Flawil, Switzerland). The solution was delivered to the water-cooled nozzle (0.7 mm liquid ori-

fice internal diameter) at a flow rate of 3 mL/min, sprayed at an inlet air temperature (T_{inlet}) of 90 or 120°C and an outlet air temperature of 40-43°C or 60-62°C. The drying air volumetric flow rate was set at 35 m^3/h, and the atomizing air volumetric flow rate at 600 L/h. The produced powders were collected through a high-efficiency cyclone in a glass container, and stored at -20°C.

2.2.5. Morphological analysis

The powder samples were mounted on the brass stub using double-sided adhesive tape and were made electrically conductive by gold coating (18 nm/min) in vacuum (4 kPa) using the MSP-mini Magnetron Sputter (Vacuum Device Co., Ltd., Ibaraki, Japan) for 45 s at 26 mA. The scanning electron microscope (SEM) images were analyzed at 15 kV accelerating voltage with an image analysis system (Miniscope® TM3000, Hitachi High-Technologies Corporation, Tokyo, Japan). Micrographs were presented at 6000x magnification.

2.2.6. Particle size measurement

The particle size measurements were examined with a Sympatec HELOS/RODOS (Sympatec GmbH, Clausthal-Zellerfeld, Germany) equipped with a vibratory feeder and R1 lens (0.1-35 µm). The primary pressure was set manually using the adjustment valve in the range of 0.2-4.5 bar, and three measurements were recorded using freshly loaded powder. The particle size distribution (x10, x50 and x90) was calculated using the Fraunhofer theory.

2.2.7. Size exclusion high-performance liquid chromatography (SE-HPLC)

The size exclusion chromatography was used to evaluate the amount of soluble protein aggregates in the spray-dried powders after dissolution. The analysis was performed on a Waters HPLC system with a TSK3000SWXL column (300 x 7.8 mm, Tosoh, Tokyo, Japan), and UV detection was done at 280 nm. The mobile phase consisted of 0.1 M disodium hydrogen phosphate dehydrate and 0.1 M sodium sulfate, and was adjusted with phosphoric acid to pH 6.8. The flow rate was 1 mL/min and the injection volume was 50 µL with a protein concentration of approximately 5 mg/mL. The samples were analyzed in duplicates.

2.2.8. Circular dichroism (CD) measurement

CD measurements were performed with a J-820 spectropolarimeter (Jasco, Tokyo, Japan). The temperature of the sample solution in the cuvette was controlled at 25.0°C by a Peltier PTC-423 L thermo-unit (Jasco). The path length of the optical quartz cuvette was 1.0 mm for far-UV range CD measurements conducted at 200 to 260 nm, and 10 mm for near-UV range CD measurements conducted at 250 to 350 nm. The sample concentration for the far-UV and near-UV range was 5 and 40 µM in 5 mM Tris-HCl (pH 8.0), respectively. The data were expressed as the molar residue ellipticity (θ).

2.2.9. Dissolution testing

Dissolution testing of the spray-dried telmisartan/L-PGDS complex in several media

[simulated gastric fluid (SGF) including pepsin, McIlvaine buffer pH 5.0, and 0.05 M phosphate buffer pH 6.8] was implemented for 60 min at 37°C with a miniaturized dissolution apparatus (µDiss Profiler™, pION, Billerica, Massachusetts, USA) due to the lack of sample availability. The applied amount of telmisartan was 0.67 mg in 15 mL of test medium, which is equivalent in concentration to 40 mg of telmisartan in 900 mL of test medium. The commercial product was milled by mortar and pestle before the testing. An appropriate amount of the produced powder was added to the test medium directly on stirring with a magnetic stirrer at 300 rpm. The sample solution was withdrawn at sampling points, and the amount of telmisartan assayed with the HPLC method as described previously in 2.2.3.

2.2.10. In vitro digestion study

2.2.10.1. Preparation of biorelevant media

The fasted state-simulated gastric fluid (FaSSGF) and fasted state simulated intestinal fluid (FaSSIF) were prepared from the simulated intestinal fluid (SIF) powder (Biorelevant.com, Croydon, Surrey, UK) [51, 52].

2.2.10.2. Digestion study in FaSSGF

Aliquots (180 µL) of FaSSGF including 3.2 mg/mL pepsin were placed in 1.5 mL microcentrifuge tubes and incubated in a water bath at 37°C for 180 min. L-PGDS of 20 µL (3.8 mg/mL) was added to each of the FaSSGF vials to start the digestion reaction. NaOH (3.75 N) of 20 µL was added to each vial to stop the reaction. The samples were

then mixed with loading dye containing β-mercaptoethanol and resolved on sodium dodecyl sulfate-polyacrylamide gel (SDS-PAGE). Proteins were visualized by Coomassie Brilliant Blue staining.

2.2.10.3. Sequential digestion study (FaSSGF followed by FaSSIF)

L-PGDS of 20 μL (3.8 mg/mL) was added to each of the 180 μL of FaSSGF including 3.2 mg/mL pepsin vials, and the digestion reaction was performed at 37°C for 60 min. The digested solution of 100 μL was added to each of the 900 μL of FaSSIF with 10 mg/mL pancreatin. Each sample was incubated at 37°C for 240 min, and the digestion reaction was stopped by placing the tube in a boiling water bath for 5 min. The samples were then mixed with loading dye with β-mercaptoethanol. The proteins were separated by SDS-PAGE and visualized by Coomassie Brilliant Blue staining.

2.2.11. Pharmacokinetic study

The spontaneously hypertensive rats (SHR, nine weeks of age, male, Japan SLC Inc., Shizuoka, Japan) were housed under a 12-h light-dark schedule with free access to food and water for one week to recover from the stress of transportation. All procedures used in this study were complied with policies of the Osaka Prefecture University Animal Care and Use Committee (Approval No. 25-80).

2.2.11.1. Sample administration and blood sampling

Eighteen rats were randomly divided into three groups (n = 6, per group). Jet-milled

telmisartan was administered orally along with PBS (phosphate buffer saline, pH 7.4) suspension at a dose of 4 mg/kg telmisartan (5 mL/kg). The commercial product and telmisartan/L-PGDS complex were administered orally as a phosphate buffer solution (PBS) (pH 7.4) solution just after the preparation at a dose of 4 mg/kg telmisartan (5 mL/kg). The dose of telmisartan used in this study was a 40 mg dose per 60 kg of human body weight, which was based on calculation with body surface area as a factor to convert a dose for translation from rats to humans [53].

The blood samples (300 μL) were collected from the tail vein of rats at pre-dose (0 h), 0.25, 0.5, 1, 2, 4, 8, 12, 24, and 48 h after the oral administration. The collected samples were centrifuged at 10,000 rpm for 5 min to harvest serum, and stored at -20°C until further analysis.

2.2.11.2. Liquid chromatography-mass spectrometry (LC-MS)/MS analysis of serum concentration of telmisartan

Thawed 50 μL of serum and 50 μL of Probenecid solution as internal standards were mixed, and 200 μL of acetonitrile/methanol/water (50/45/5, v/v) was added for protein precipitation. After the centrifugation at 4,000 rpm for 5 min, 200 μL of supernatant was mixed with 200 μL of 10 mM ammonium acetate/acetonitrile (50/50,v/v), and analyzed with LC-MS/MS. In the HPLC part, using an Agilent 1100 series HPLC (Agilent, Santa Clara, California, USA) equipped Xbridge BEH 300 C18 (2.1 mm I.D. x 50 mm length, 3.5 μm, Waters Corp.), the sample was separated under a gradient condition that consisted of 10 mM ammonium acetate (Solvent A) and acetonitrile (Solvent B) at a flow rate of 0.4 mL/min. The gradient condition was configured as 0-1.0 min; 50% Sol-

vent A, 1.0-2.0 min; 50-10% Solvent A, 2.0-3.0 min; 10-50% Solvent A, and 3.0-5.0 min; 50% Solvent A.

The separated sample was placed into the MS/MS part API4000™ (AB SCIEX, Framingham, Massachusetts, USA) equipped with TurboIonSpray as an ion source. Telmisartan and Probenecid were monitored by multiple reactions monitoring of the transitions of m/z 516.1 → 276.3 and m/z 286.2 → 243.8, respectively.

2.2.12. Pharmacodynamic study

Male SHR (nine weeks of age, Japan SLC Inc.) were housed under a 12-h light-dark schedule with free access to food and water for one week to recover from the stress of transportation. All procedures used in this study complied with the institutional policies for the care and use of laboratory animals (Approval No. 140328A).

Twenty-four rats were randomly assigned to four groups (n = 6, per group) based on the systolic blood pressure (SBP). The same samples, as in the pharmacokinetic study, were orally administered and PBS (pH 7.4) was administered as a control. The SBP and heart rate were measured by the noninvasive tail-cuff method using MK-2000 (Muromachi Kikai Co., Ltd., Tokyo, Japan) at pre-dose (0 h), 0.5, 1, 2, 4, 8, 12, 24, and 48 h after the oral administration.

2.2.13. Statistical analysis

The data were statistically evaluated using one-way ANOVA followed by Dunnett's test. The results were considered significant at 5% significance level ($p < 0.05$).

2.3. Results

2.3.1. Solubility study

2.3.1.1. Evaluation of solubility enhancement by L-PGDS

Firstly, I evaluated the solubility enhancement of telmisartan by the addition of L-PGDS in the several kinds of buffer medium (Table 2). The solubility of telmisartan (0.26-3.12 μg/mL) was significantly enhanced approximately by 260-fold (816-834 μg/mL) with 25 mg of L-PGDS in the all evaluated mediums, and there was no effect of buffer species and ion strength on the solubility enhancement.

Table 3 Solubility of telmisartan at 37°C in different pH buffers in the presence of L-PGDS.

Medium	25 mg L-PGDS	μg/mL
SGF (pH 1.2)	-	257
McIlvaine buffer (pH 5.0)	-	0.26
	+	826
50 mM phosphate buffer (pH 6.8)	-	0.22
	+	834
5 mM Tris-HCl buffer (pH 8.0)	-	3.12
	+	816
Sorenson's Buffer (pH 9.0)	-	44.1

SGF, stimulated gastric fluid; L-PGDS, lipocalin-type prostaglandin D synthase

2.3.1.2. Determination of complexation rate

I checked the solubility profiles of telmisartan in 5 mM Tris-HCl buffer solution (pH 8.0) with the various amounts of L-PGDS at 37°C (Table 3). The solubility of telmisartan increased with the rise in the levels of L-PGDS, and a linear increase was observed after incubation for 120 min ($r^2 = 0.987$). From the solubility profile, the apparent stability constant was calculated as 1.73×10^5 M^{-1}, and the complexation rate was approxi-

mately 1:1 molar ratio. On the other hand, in the case of the preparation of the telmisartan and L-PGDS complex carried out at room temperature, the same enhanced concentration of telmisartan was observed after 24 hours (Fig. 8). With change in the volume of L-PGDS solution from 1 to 100 mL that included the same amount of L-PGDS, no significant difference was observed in the solubility enhancement of telmisartan as compared with the case at 37°C (Fig. 9). Based on this result, I decided to prepare the telmisartan/L-PGDS at 37°C for further studies, and 10-25 mg/mL of L-PGDS was employed for the spray-drying process.

Table 4 Solubility profile of telmisartan with several concentrations of L-PGDS in 5 mM Tris-HCl buffer (pH 8.0).

	Solubility (μM)			
L-PGDS	0	270	800	1330
Telmisartan	45	474	1120	1590

L-PGDS, lipocalin-type prostaglandin D synthase

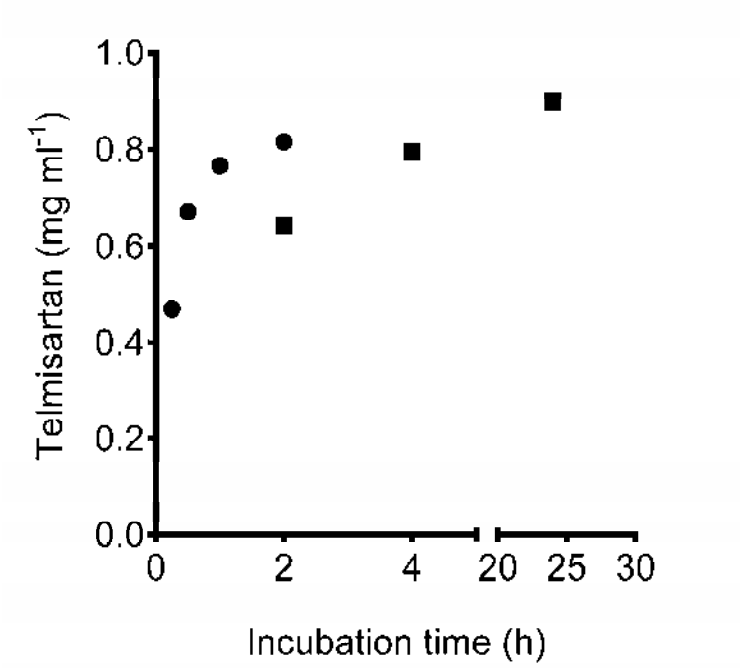

Figure 8 The influence of temperature on the solubility enhancement of telmisartan by the addition of L-PGDS. **l** : 37°C and **n**: room temperature.

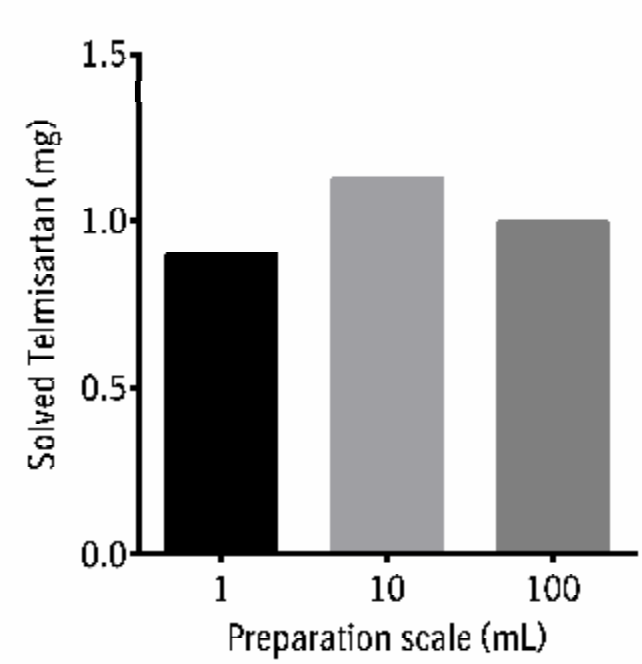

Figure 9 The influence of preparation scale on the solubility enhancement of telmisartan by the addition of 25 mg of L-PGDS.

2.3.2. Physical characterization of spray-dried telmisartan/L-PGDS complex

2.3.2.1.Spray-drying process of L-PGDS solution

All spray-drying runs showed a high yield of 50-90%. Only a small amount of powdery deposit was observed, and the inside wall of the drying chamber was found to be clean. Therefore, the marked particle loss was mainly caused by fine particles passing through the cyclone into the exhausted air. The dried particles were obtained from the cyclone and collecting vessel.

2.3.2.2.Morphological and particle size analyses

The surface morphology of the spray-dried L-PGDS powder and spray-dried telmisartan/L-PGDS complex powder was observed with SEM (Fig. 10). Jet-milled telmisartan was the agglutinate mixture of flattened fine particles with a wide size distribution (x10 = 0.18 μm, x50 = 1.30 μm, x90 = 5.05 μm, Fig. 10A). The spray-dried L-PGDS and telmisartan/L-PGDS complex at 90°C of T_{inlet} had a smooth surface and typical spherical shape, with a narrow size distribution (x10 = 0.26 μm, x50 = 2.60 μm, x90 = 6.16 μm, Fig. 10B and C). However, in the case of the powder spray-dried L-PGDS at 120°C of T_{inlet}, dimple-type particles were observed (Fig. 10D).

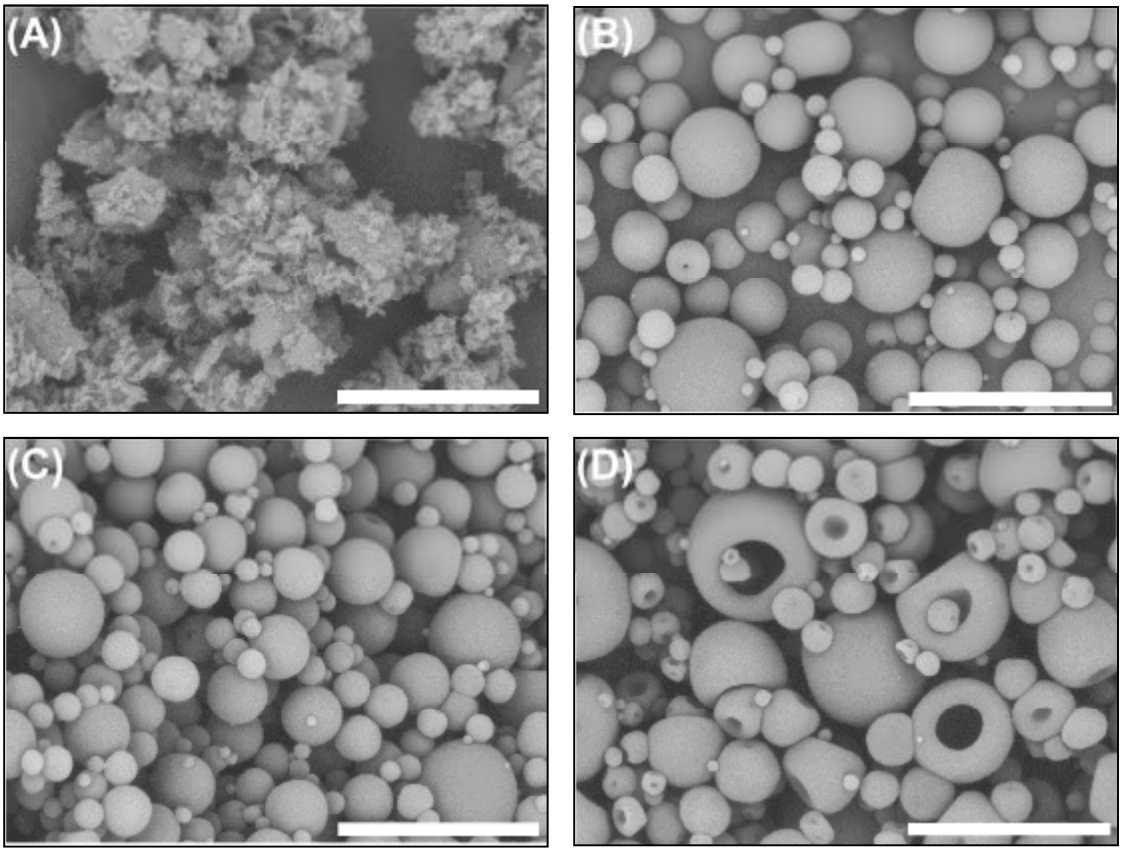

Figure 10 SEM images of (A) jet-milled telmisartan, (B) spray-dried L-PGDS powder (T_{inlet} = 90°C), (C) spray-dried telmisartan/L-PGDS complex powder (T_{inlet} = 90°C), and (D) spray-dried L-PGDS powder (T_{inlet} = 120°C). Each bar represents 10 μm.

2.3.2.3. Reconstitution of spray-dried L-PGDS

The spray-dried L-PGDS powder was reconstituted with 5 mM Tris-HCl (pH 8.0), and the reconstituted solution was applied to SE-HPLC to verify the soluble aggregate of L-PGDS. The chromatogram indicated only a single peak of L-PGDS, and the soluble aggregation was not observed in the reconstituted L-PGDS solution (Fig.11). The structure of reconstituted L-PGDS was monitored with CD measurement. The reconstituted solutions of spray-dried L-PGDS was produced at 90 and 120°C of T_{inlet} that had the same spectrum as the control in the far- and near-UV regions, respectively (Fig. 12A and B). These results showed that the secondary and tertiary structures of L-PGDS were not altered by the spray drying.

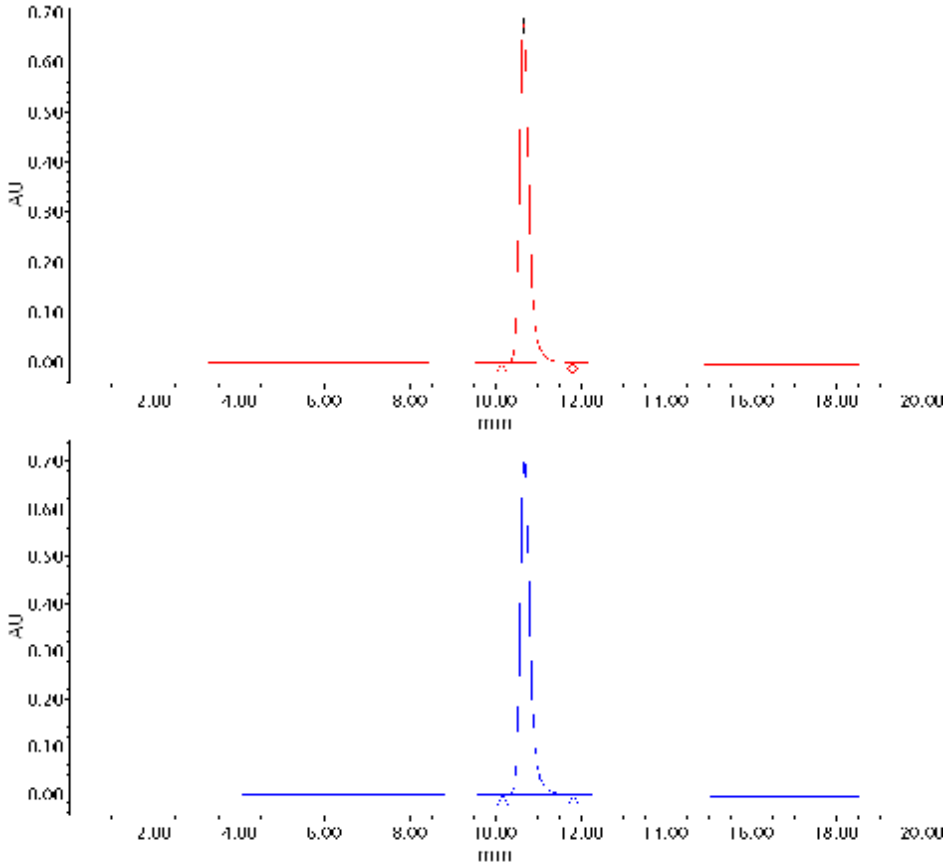

Figure 11 Size exclusion chromatogram of reconstituted L-PDGS dried at T_{inlet} = 90°C (red) and reconstituted L-PGDS dried at T_{inlet}= 120°C (blue).

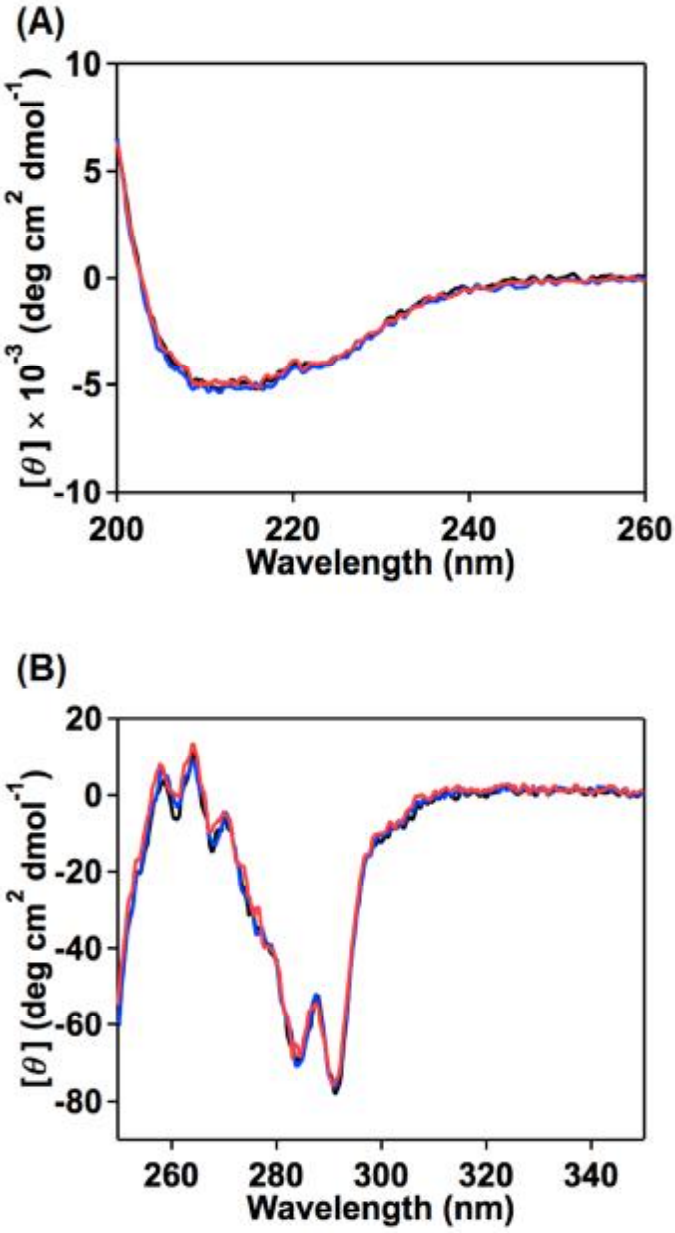

Figure 12 CD spectra in (A): far-UV and (B): near-UV region of intact L-PGDS solution (black), reconstituted L-PDGS dried at T_{inlet} = 90°C (blue) and reconstituted L-PGDS dried at T_{inlet} = 120°C (red).

2.3.2.4. In vitro dissolution behavior

The small-scale dissolution testing was performed to evaluate the *in vitro* dissolution behavior of the spray-dried telmisartan/L-PGDS complex (Fig. 13). The jet-milled telmisartan and commercial product were measured as control for the telmisartan/L-PGDS complex. The dissolution level of jet-milled telmisartan in SGF with pepsin (pH 1.2) was 90% of the applied total amount of the drug (Fig. 13A), while the solubility at pH 5.0 and 6.8 was 4-5% at 60 min, respectively (Fig. 13B and C). The commercial product improved the dissolution of telmisartan, and a 100% dissolution level was achieved at both the pH 1.2 and 6.8 (Fig. 13A and C). However, the maximum drug release from the commercial product was only 16% at pH 5.0 at 60 min (Fig. 13B). In contrast, the complex formulation significantly enhanced the release of telmisartan, and achieved 100% dissolution within 10 min in all the evaluated test media. Furthermore, the L-PGDS formulation maintained the enhanced dissolution of telmisartan in the presence of pepsin for up to 2 h (Fig. 13A).

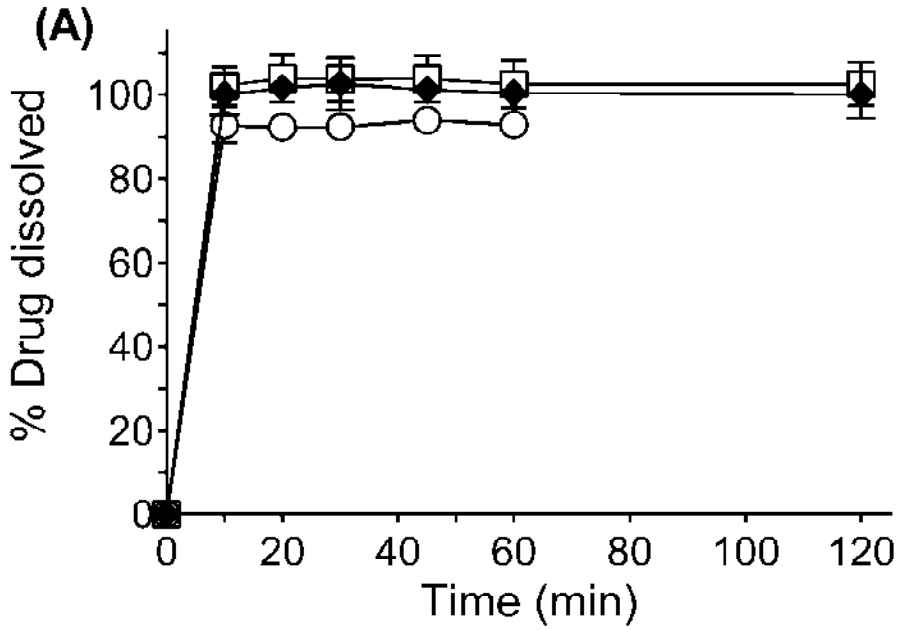

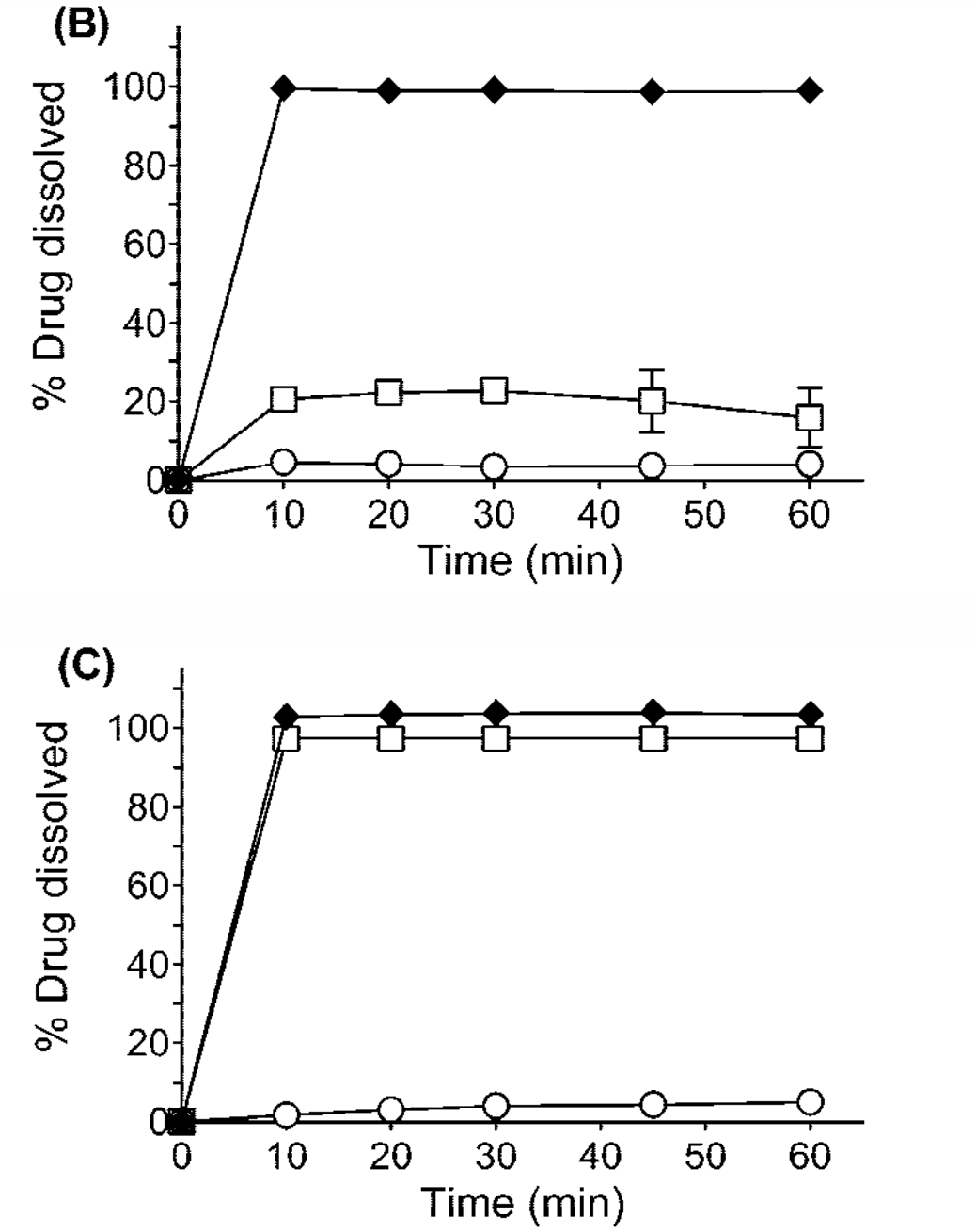

Figure 13 Dissolution profiles of telmisartan formulations in (A) SGF with pepsin (pH 1.2), (B) McIlvaine buffer (pH 5.0), and (C) 0.05 M phosphate buffer (pH 6.8). ○: telmisartan, □: commercial product, and ¿: spray-dried telmisartan/L-PGDS complex. The concentration of telmisartan: 0.044 mg/mL. Each bar represents the mean ± SD of three independent experiments.

2.3.2.5. In vitro digestibility of L-PGDS under simulated gastrointestinal conditions

An *in vitro* digestion study was implemented with the simulated gastrointestinal medium to verify the stability of L-PGDS in the gastrointestinal environment (Fig. 14). Although the minor and time-dependent digestion of L-PGDS under the simulated gastric condition was observed, the major structure of L-PGDS was stable in the environment for 180 min (Fig. 14A). The structure of L-PGDS was completely changed to the digested form at 30 min after exposure under the gastric conditions. On the other hand, the digested L-PGDS in FaSSGF was rapidly degraded in the simulated intestinal environment, and there was no corresponding band for L-PGDS at 1 min after the digestion in FaSSIF (Fig. 14B).

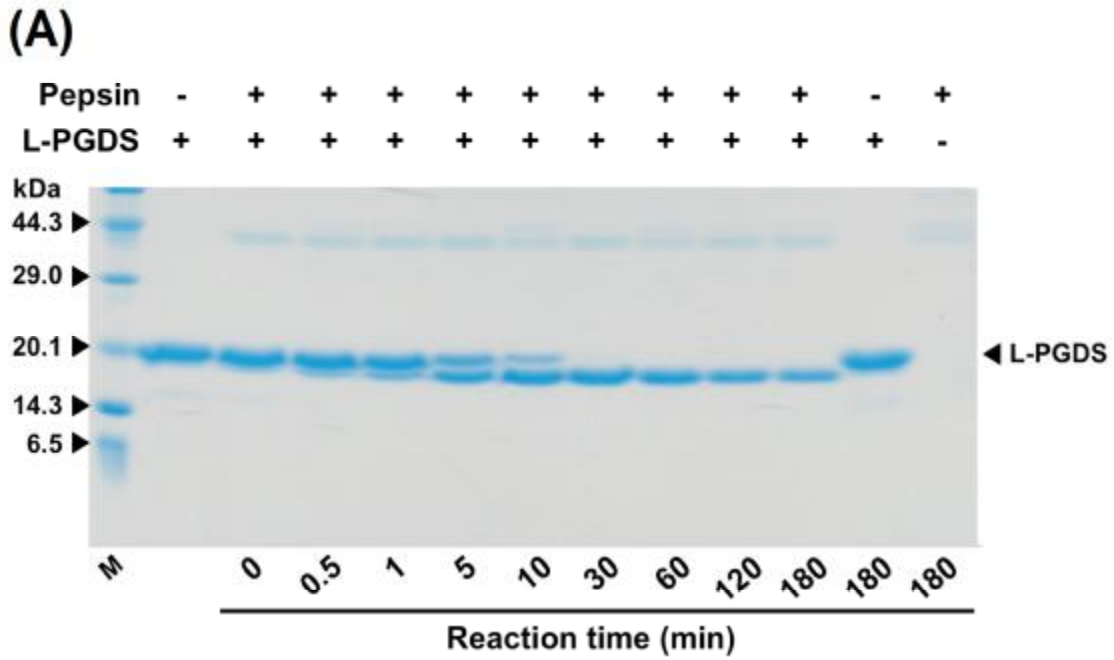

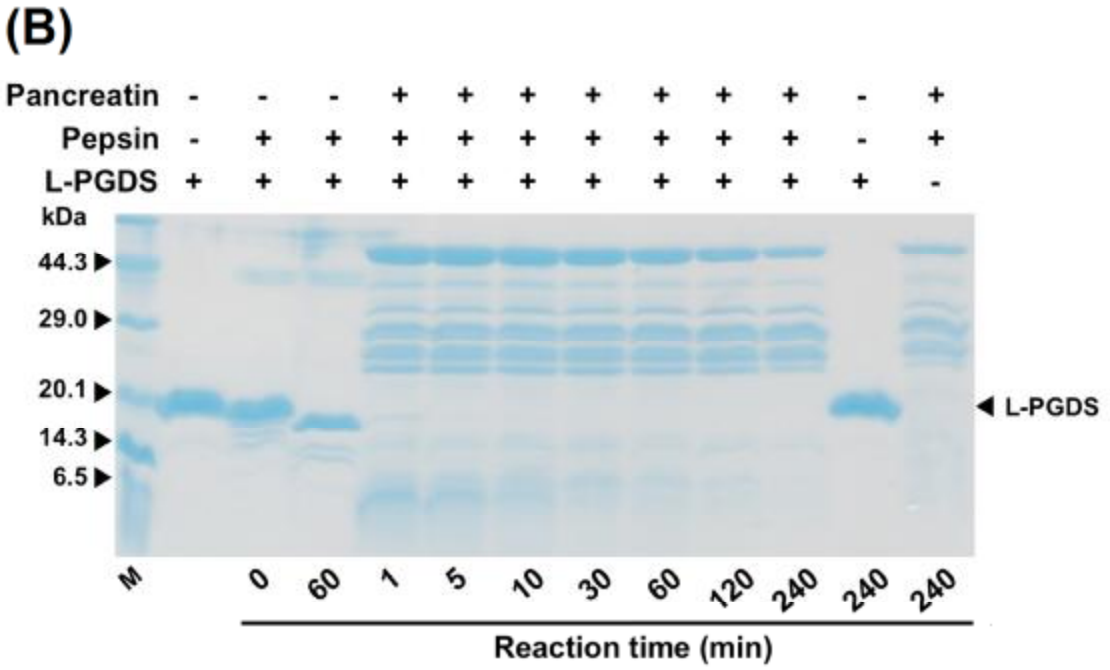

Figure 14 SDS–PAGE analysis of the (A) *in vitro* digestion study in FaSSGF and (B) sequential digestion study in FaSSGF followed by FaSSIF. M: molecular weight marker. Digestion reaction was performed at 37°C.

2.3.3. In vivo evaluation of solubilized formulation of telmisartan with L-PGDS complex

2.3.3.1. Pharmacokinetic study

The concentration of telmisartan in serum was quantified to evaluate the *in vivo* behavior of the orally administered telmisartan/L-PGDS complex with SHR (Fig. 15). The calculated pharmacokinetic parameters are listed in Table 3. The jet-milled telmisartan showed the lowest values for all parameters, and telmisartan was not detected at 48 h after the oral administration. The telmisartan/L-PDGS complex significantly improved the *in vivo* behavior of telmisartan in the area under the serum concentration-time curve from 0 to 48 h ($AUC_{0\text{-}48h}$), maximum concentration (C_{max}), and time to maximum con-

centration (T_{max}). Especially, $AUC_{0\text{-}48h}$ of the complex formulation was 5.9-fold in that of the jet-milled telmisartan, and T_{max} of the complex formulation was significantly shorter than in jet-milled telmisartan and the commercial product. The significant difference for an elimination of half-life ($T_{1/2}$) in these three formulations remained unobserved.

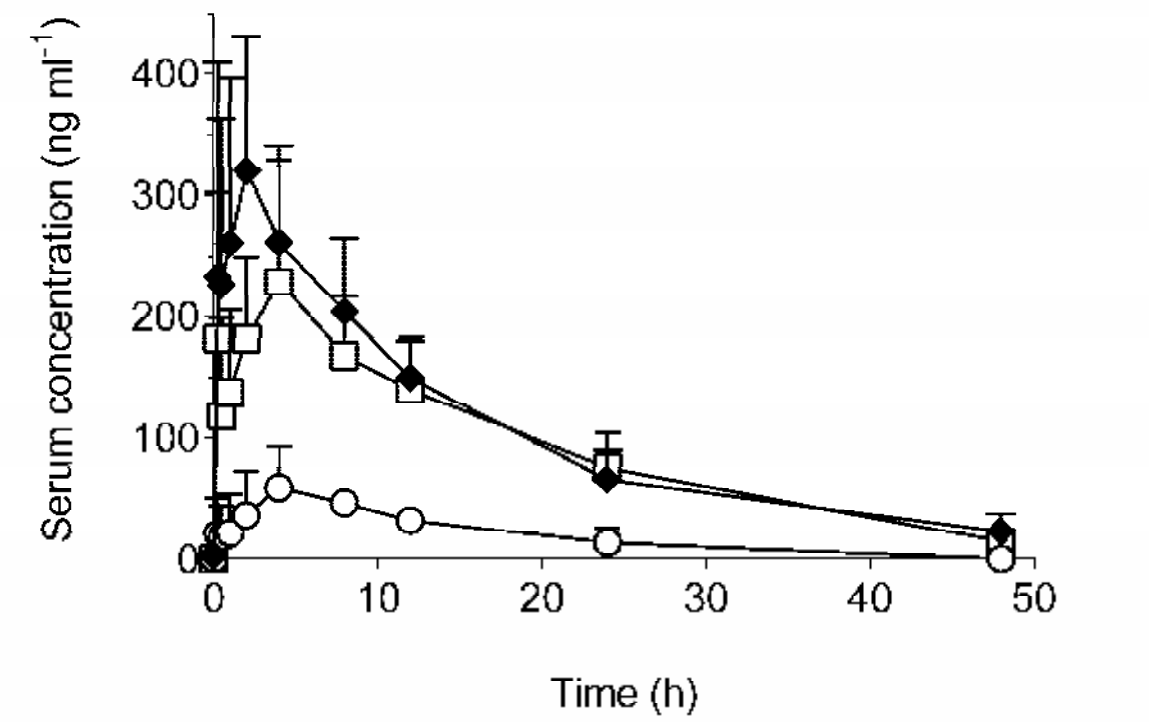

Figure 15 The time-profile of the serum concentration of telmisartan in SHR after oral administration (4 mg/kg telmisartan). ○: jet-milled telmisartan, □: commercial product, and ¿ : telmisartan/L-PGDS complex. Each bar represents the mean ± SD of six independent experiments.

Table 5 Pharmacokinetic parameters for telmisartan formulations after oral administration.

	AUC (ng h/ml)	C_{max} (ng/ml)	T_{max} (h)
Jet-milled telmisartan	947 ± 435	66.0 ± 27.4	4.0
Commercial product	4,820 ± 836*	296 ± 70.5*	4.0
Telmisartan/L-PGDS complex	5,610 ± 548*	348 ± 100*	1.3

L-PGDS, lipocalin-type prostaglandin D synthase

*: Significant difference from jet-milled telmisartan ($P < 0.05$)

Values (AUC, C_{max}) are expressed as the mean ± SD of six experiments.

2.3.3.2. Pharmacodynamic study

Next, I investigated the antihypertensive effect of the complex formulation of telmisartan/L-PGDS, and the effect was compared with jet-milled telmisartan and the commercial product by monitoring the change in the systolic blood pressure (ΔSBP) after a single oral administration (Fig. 16). An increase in SBP at 0.5 h after the oral administration was observed in each sample group, and the sample group data were analyzed in five subjects. All three formulations showed a comparable reduction of SBP (Fig. 16A). However, based on the calculated area under the curve of ΔSBP, the commercial product and telmisartan/L-PGDS complex formulation had a tendency to reduce SBP more than the jet-milled telmisartan as compared with the control (Fig. 16B). In addition, the commercial product and telmisartan/L-PGDS complex caused an immediate decrease in SBP (jet-milled telmisartan: - 11.4 ± 5.5 mmHg, commercial product: - 17.4 ± 4.7 mmHg and telmisartan/L-PGDS complex: - 18.2 ± 6.7 mmHg at 0.5 h after administration). Although the effect of jet-milled telmisartan returned to the basal level at 48 h after the administration, the commercial product and complex formulation retained the effect (jet-milled telmisartan: 5.6 ± 6.3 mmHg, commercial product: - 4.6 ± 7.9 mmHg and telmisartan/L-PGDS complex: - 8.4 ± 6.3 mmHg at 48 h after administration). Moreover, there was no significant change in the heart rate as compared to the control along with all formulations (Fig. 17). These results demonstrated that the telmisartan/L-PGDS complex possessed drug potency almost equal to the commercial product.

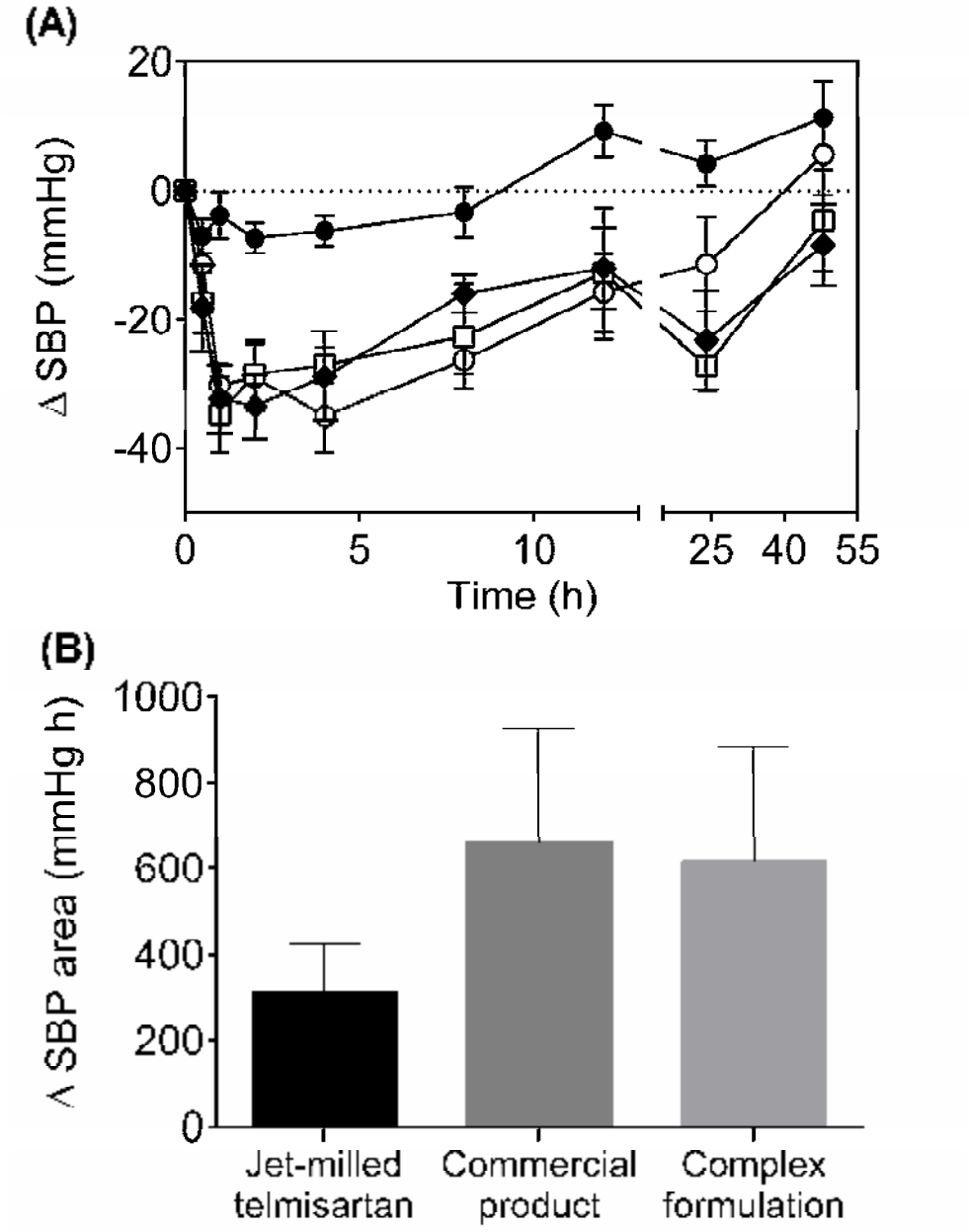

Figure 16 Change in systolic blood pressure (ΔSBP). (A): time-profile of ΔSBP after oral administration (4 mg/kg telmisartan). ●: control, ○: jet-milled telmisartan, □: commercial product, and ¿: telmisartan/L-PGDS complex. The bar of the control is expressed as mean ± SE of six independent experiments, and bars of the others represent the mean ± SE of five independent experiments. (B) Comparison of the area under the curve of ΔSBP (mmHg h).

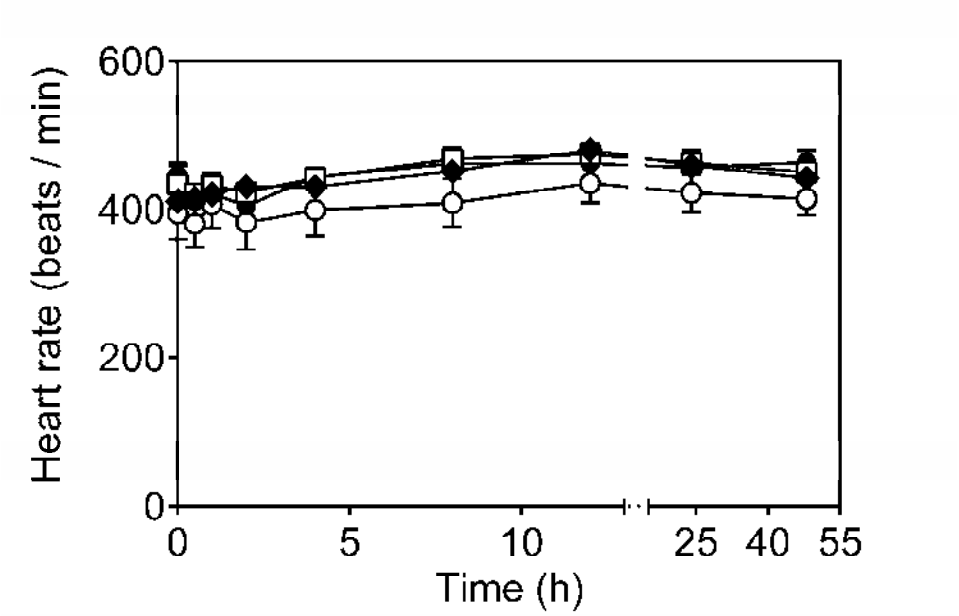

Figure 17 Change of heart rate for sample administered rats. ●: control, ○: jet-milled telmisartan, □: commercial product, and ¿: telmisartan/L-PGDS complex. The bar of the control is expressed as mean ± SE of six independent experiments, and bars of the others represent the mean ± SE of five independent experiments.

2.4. Discussion

In this chapter, I showed that the solubility of telmisartan is enhanced in the presence of L-PGDS and that the complex formulation is the first order increase with respect to the amount of L-PGDS with the simple preparation method (Table 4). In addition, the *in vitro* dissolution study revealed that the telmisartan/L-PGDS complex showed a significantly faster dissolution rate than the jet-milled telmisartan, and reached 100% in the physiological pH range. Interestingly, the complex formulation improved the extent of dissolution for telmisartan, and the improved solubility was maintained in SGF (Fig. 13A). Moreover, the main structure of L-PGDS should be stable under the simulated gastric conditions, but low-level digestion of L-PGDS with pepsin was observed (Fig.

14A). The digested fragment might be the flexible fragment in both the N- and C-terminal regions [16], and the central antiparallel β-barrel and long α-helix region that form the hydrophobic cavity would be maintained. These results suggest that the complex formulation is maintained in a low pH environment in the presence of pepsin. The pH environment of the gastrointestinal tract varies due to several factors, such as aging, food, and the influence of administered drugs [54-56]. The variation in pH resulted in variable bioavailability and unexpected drug absorption. Hence, this consistent dissolution behavior under physiological pH conditions is considered to be beneficial.

The spray-drying process robustly produced the stable dried protein powder that maintained the secondary and tertiary structures with the standard process parameters, such as T_{inlet}, the atomizing air volumetric flow rate, and liquid concentration (Fig. 12). In addition, the narrow particle size distribution of the produced powder demonstrated that the spray-drying process of L-PGDS formulation achieved the atomizing of well-dispersed droplet without the additives, such as surfactants, to prevent the generation of aggregates. There was a morphologic difference in the dried particles due to the increase of T_{inlet} (Fig. 10D). The rate of droplet evaporation may affect the morphological properties of the particles [57]. A fast drying rate would promote the formation of a more viscous film in the initial phase of drying. The film tends to burst because of the rapid increase in the water pressure inside the droplet. Therefore, the fast drying conditions result in a large fraction of the particles containing dimples or holes. In general, the spray-drying process may alter the secondary structure of protein because of the removal of water molecules that are required to form hydrogen bonds to stabilize the structure. This can be prevented by adding excipients, e.g., carbohydrates, which are capable of forming hydrogen bonds with the protein [58-60]. In this study, the produced powder

was stored at -20°C until each analysis, for the precise evaluation of the characteristics without the potential degradation, derived from the temperature and humidity.

In the pharmacokinetic study, the telmisartan/L-PDGS complex significantly enhanced the *in vivo* behavior of jet-milled telmisartan, and, in particular, $AUC_{0\text{-}48h}$ and C_{max} were enhanced 5.9- and 5.3-fold, respectively (Table 5). T_{max} of the complex formulation was significantly shorter than jet-milled telmisartan and the commercial product. The dissolution profile of the commercial product in McIlvaine buffer pH 5.0 showed the incomplete dissolution and moderate precipitation behavior after supersaturation (Fig. 13B). On the other hand, the *in vitro* sequential digestion experiments revealed the rapid release of telmisartan from the telmisartan/L-PGDS complex by the digestion of L-PGDS in the simulated intestinal environment (Fig. 14B). Therefore, the significant shorter T_{max} of the complex formulation was considered as the release of telmisartan from the complex formulation that was faster than the commercial product. These results suggested that the spray-dried complex formulation enhanced the oral exposure and absorption rate.

The pharmacodynamic study showed no significant difference in the reduction of SBP between all the formulations (Fig. 16A). The administered dose may achieve the dose range for a saturated reduction effect. Therefore, a comparison study with lower dose strength could reveal the difference between formulations for the reduction of SBP. However, the complex formulation led to the improvement of the antihypertensive effect of comparing the total ΔSBP area with jet-milled telmisartan (Fig. 16B). One of the clinical advantages of telmisartan is its long-acting effect due to the delayed dissociation from angiotensin II type-1 receptor [43]. The complex formulation prolonged the reduction effect of API as well as the commercial product that was observed at 48 h after the

oral administration. This prolonged effect corresponded to the results obtained from the pharmacokinetic study that detected telmisartan in the serum at 48 h after the administration of telmisartan/L-PGDS formulation. In addition, the prolonged effect of telmisartan can achieve a significant antihypertensive effect without induction of any rebound phenomenon due to the repeated dosing [61].

The results of animal studies suggested that L-PGDS delivers telmisartan to the absorption site while maintaining the complex formed from protein in an adverse environment (i.e., low pH and presence of protease).

2.5. Conclusions

The solubilization of telmisartan was achieved by a simple complex formulation method involving L-PGDS. The dried powder of the solubilizing formulation was successfully produced by spray-drying technique. The solubilizing effect of L-PGDS demonstrated a consistent *in vitro* dissolution profile in the physiological pH range and *in vivo* behavior comparable to that of the commercial product. This study demonstrated that L-PGDS is a potent drug-delivery carrier for the oral solid formulation. The drug-delivery system using biodegradable material can be an alternative approach for the current investigation of solubilizing techniques, such as supersaturated formulations.

3
Development of pH-independent drug release formulation using L-PGDS

3.1. Introduction

In the case of oral administration of ionizable compounds, there is a significant change in the solubility of weak basic compounds due to the pH shift in the transition from the stomach to the small intestine. Although the weak bases are soluble in the acidic environment of the stomach, the solubility is markedly decreased in the higher pH environment of the small intestinal fluids. The drug has to be present in the dissolved form in the small intestine for absorption. Hence, solubilization at a low pH environment of the stomach is a key process for the absorption of weak basic drugs [62]. However, the pH environment in the gastrointestinal tract varies on the low-level secretion of gastric acid due to several factors, for e.g., aging, infection with *Helicobacter pylori*, and influence of administered drugs, such as histamine H_2 receptor antagonists and proton pump inhibitors [55, 63, 64]. Hence, the variable bioavailability and unexpected drug absorption of weak basic drugs occur due to the pH variation of gastrointestinal compartments.

Dipyridamole (Fig. 18) is a phosphodiesterase inhibitor that has been suggested to increase the intracellular levels of cyclic adenosine monophosphate (cAMP) and cyclic guanine monophosphate (cGMP), and dipyridamole has been clinically used for antiplatelet therapy and platelet-mediated thrombotic disease [65]. Dipyridamole is a weak basic compound with a reported pK_a of 6.4 and shows markedly pH-dependent solubility (Fig.19) [66]. The previous study showed that the patients with an elevated gastric pH

induced by pretreatment with lansoprazole, a widely used proton pump inhibitor, exhibited decreased absorption of dipyridamole [67]. Several approaches, such as inclusion with cyclodextrin, a self-microemulsifying drug delivery system (SMEDDS), solid dispersion, and microenvironmental pH-modulation with a pH modifier, have been investigated to improve the absorption behavior of dipyridamole [68-71]. It has been reported that cyclodextrin may reduce drug absorption as opposed to solubility enhancement as a result of the decrease in the drug's free fraction available for absorption [12-14]. For the application of dipyridamole in a clinical stage, however, marked efforts are necessary for optimization of the formulation and manufacturing process and alleviation of concerns over the inadequate stability of the product. In chapter 1, the produced solid-state telmisartan/L-PGDS complex formulation showed consistent dissolution profiles over the entire physiological pH range *in vitro*.

In this chapter, I developed a novel dipyridamole formulation using L-PGDS to improve the solubility and oral absorption behavior in the elevated gastric pH environment. The solid-state dipyridamole/L-PGDS complex formulation was produced by spray drying technique, and the physicochemical properties were characterized from the aspects of morphology, hygroscopicity, and dissolution profiles under fasted-state simulated gastric and neutral pH conditions. Finally, the pharmacokinetic behavior subsequent to oral administration of the developed formulation in rats with an elevated gastric pH following the pre-treatment with omeprazole was evaluated, and compared with the intact API.

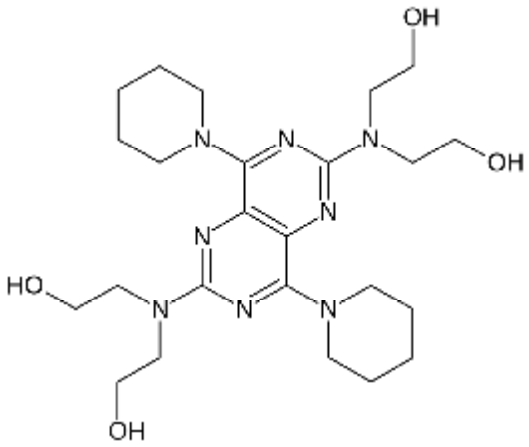

Figure 18 Chemical structure of dipyridamole [relative molecular mass: 504.6].

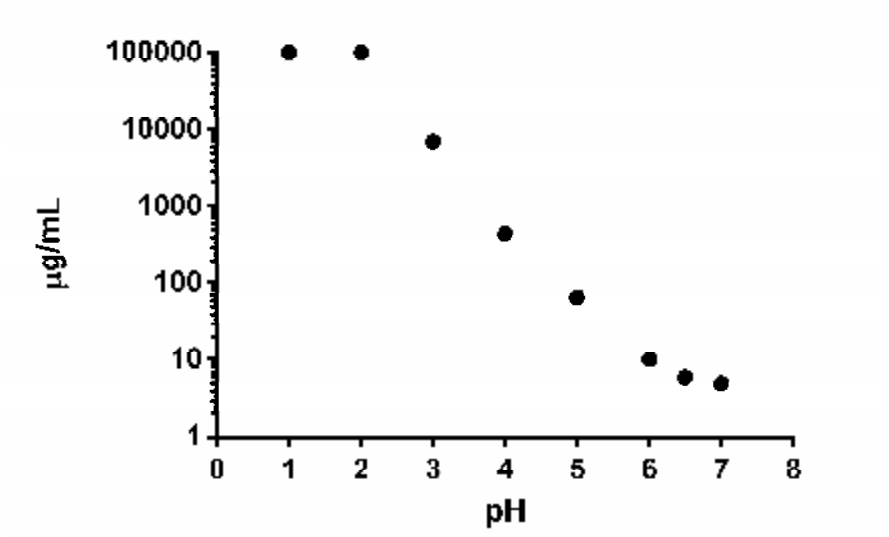

Figure 19 pH-solubility profile of dipyridamole.

3.2. Materials and methods

3.2.1. Materials

Dipyridamole was supplied by Boehringer Ingelheim GmbH & Co., KG (Ingelheim,

Germany). All other chemicals were of analytical grades.

3.2.2. Molecular docking study

The docking of dipyridamole into the crystal structure of L-PGDS was performed with AutoDock Vina program [25]. AutoDock Vina gridboxes covered the barrel of L-PGDS with approximate dimensions 18 × 18 × 18 with grid points separated by 1 Å.

3.2.3. Purification of recombinant human L-PGDS

The isolation and purification process of recombinant human C65A/C167A (ε_{280} =25,900 M^{-1} cm^{-1})-substituted L-PGDS mutant was same as described in 2.2.2 section of chapter 2.

3.2.4. Fluorescence Quenching Assays

Various concentrations of dipyridamole were successively added to L-PGDS (final concentration: 2 μM) in PBS containing 5% dimethyl sulfoxide (DMSO). After incubation at 25°C for 30 min, the intrinsic tryptophan fluorescence was measured by HITACHI F-7000 (Hitachi, Ltd., Tokyo, Japan) with an excitation wavelength of 290 nm and an emission wavelength at 340 nm. The fluorescence resonance energy transfer between tryptophan residues of L-PGDS and bound dipyridamole was monitored by the fluorescence emission between 300 and 450 nm. The dissociation constant (K_d) value for binding between dipyridamole and L-PGDS was calculated by the previously described method [26].

3.2.5. Solubility study

An excess amount of dipyridamole was weighed in a 2 mL microtube with 1 mL of aqueous solution containing several kinds of buffer medium in the presence or absence of L-PGDS. FaSSGF and FaSSIF were prepared as per the description in section 2.2.10 of chapter 2. The sealed microtubes were shaken with a Rotator RT-50 (TAITEC, Saitama, Japan) for 2 h at 37°C, followed by filtration through a 0.45 µm filter (EMD Millipore, Billerica, Massachusetts, USA). After incubation, the sample solution was diluted with methanol and centrifuged at 3,000 rpm for 10 min. Then, 5 µL of filtered supernatant (0.45 µm filter) was injected into a high-performance liquid chromatograph (HPLC, Waters Corporation, Milford, Massachusetts, USA) equipped with an Inertosil ODS-2 column (60 x 3.0 mm I.D., 5 µm, GL Sciences Inc., Tokyo, Japan) to analyze the amount of dipyridamole. A mixture of formate buffer (pH 6.5), methanol, and acetonitrile (58:24:18, v/v) constituted the mobile phase and was eluted at a flow rate of 1 mL/min. The chromatogram was monitored at 290 nm.

3.2.6. Spray drying of dipyridamole/L-PGDS complex solution

Based on the solubility study, the complex of L-PGDS and dipyridamole was prepared at 1:1 molar ratio in 5 mM Tris-HCl (pH 8.0). Tris-HCl buffer solution including the dipyridamole/L-PGDS complex was directly spray-dried to avoid the potential instability of L-PGDS caused by the long-term buffer substitution by dialysis. The complex solution was filtered through a 0.45 µm filter (EMD Millipore) before the spray-drying process. The dried L-PGDS or the dipyridamole/L-PGDS complex was prepared with Mini Spray Dryer B-290 (BÜCHI Labortechnik AG, Flawil, Switzerland). The solution was

delivered to the water-cooled nozzle (0.7 mm liquid orifice internal diameter) at a flow rate of 3 mL/min, being sprayed at a T_{inlet} of 90°C and an outlet air temperature of 40-43°C. The drying air volumetric flow rate was set at 35 m^3/h, and the atomizing air volumetric flow rate at 600 L/h. The produced powders were collected through a high-efficiency cyclone in a glass container, and stored at −20°C.

3.2.7. Morphological analysis

SEM images were obtained according to the procedure described in the section 2.2.5 of chapter 2.

3.2.8. Dynamic vapor sorption (DVS) measurements

Approximately, 10 mg of powder was weighed into a sample cup placed in the dynamic vapor sorption apparatus (DVS Intrinsic, Surface Measurement Systems Ltd., UK), and exposed to a continuous flow (200 mL/min) of carrier gas (nitrogen gas). For isotherm experiments, the sample was dried at 0% relative humidity (RH) to establish its dry mass, and the humidity was increased from 0 to 90% RH in 10% increments at 40°C.

3.2.9. Assay for dipyridamole content in complex formulation

The produced spray-dried powder of 2 mg was reconstituted in 100 µL of water, with a further addition of 900 µL of methanol for protein precipitation. After centrifugation at 15,000 rpm for 5 min, the supernatant was injected into the HPLC and analyzed according to the HPLC conditions as described in section 3.2.5.

3.2.10. CD measurement

The measurement condition was same as the section 2.2.8 of chapter 2.

3.2.11. SE-HPLC

The analytical condition of SE-HPLC was same as the description of section 2.2.7 of chapter 2.

3.2.12. Small scale dissolution testing

Dissolution testing of the spray-dried dipyridamole/L-PGDS complex in several media, such as FaSSGF (pH 1.6) and 0.05 M phosphate buffer at pH 6.8, was implemented for 60 min at 37°C with a miniaturized dissolution apparatus (μDiss Profiler™, pION, Billerica, Massachusetts, USA) due to the lack of sample availability. The applied amount of dipyridamole was 0.2 mg in 4 mL of the test medium. An appropriate amount of the produced powder was directly added to the test medium on stirring with a magnetic stirrer at 300 rpm. The real-time absorbance of the drug in media was evaluated by UV fiber optic probes (range of wavelengths: 390-420 nm, path length of probe: 10 mm), and the second derivative of the UV spectra was used to prevent signal interference from the undissolved material.

3.2.13. Pharmacokinetic study

The male SD rats (six weeks of age, Japan SLC Inc., Shizuoka, Japan) were housed

under a 12-h light-dark schedule with free access to food and water for one week to recover from the transportation stress. All procedures used in this study complied with policies of the Osaka Prefecture University Animal Care and Use Committee (Approval No. 27-111).

3.2.13.1. Sample administration and blood sampling

Sixteen rats were randomly divided into four groups (n = 4 per group). Two groups were pretreated with 30 mg/kg of omeprazole suspension (1 mL/kg by oral administration) to elevate the gastric pH [72]. Dipyridamole was administered orally as a phosphate buffer solution (PBS, pH 6.8) suspension at a dose of 7.5 mg/kg dipyridamole (5 mL/kg). The dipyridamole/L-PGDS complex was administered orally as a PBS just after the preparation at a dose of 7.5 mg/kg dipyridamole (5 mL/kg). In this study, 75 mg of dipyridamole dose was used for a 60 kg human, based on a calculation using the body surface area as a factor to convert the dose from rats to humans [53]. Blood samples (200 µL) were collected from the tail vein at 0.25, 0.5, 1, 1.5, 2, 4, 8, 12, and 24 h after oral administration. The collected samples were centrifuged at 10,000 rpm for 5 min to harvest plasma and stored at −20°C until further analysis.

3.2.13.2. LC-MS/MS analysis of plasma concentration of dipyridamole

Fifty microliters of thawed plasma and 25 µL of ketoconazole solution as internal standards, and 50 µL of methanol/water (90:10, v/v) were mixed, and 500 µL of ace-

tonitrile was added for protein precipitation. After centrifugation at 15,000 rpm for 5 min, 200 µL of supernatant was transferred to an evaporation tube. The supernatant was evaporated to dryness in SPD2010 (Thermo Fisher Scientific Inc., Waltham, Massachusetts, USA) at 45°C for 90 min. After being dried, the residue was reconstituted in methanol/0.1% formic acid (30:70, v/v) and analyzed by LC-MS/MS. In the HPLC part, using an Ultimate 3000 series HPLC (Thermo Fisher Scientific Inc.) equipped with Symmetryshield RP8 (2.1 mm I.D. x 50 mm length, 3.5 µm, Waters Corp.), the sample was separated under a gradient condition consisting of 0.1% formic acid in water (Solvent A) and 0.1% formic acid in methanol (Solvent B), at a flow rate of 0.5 mL/min. The gradient condition was configured as 0-0.5 min; 60% Solvent A, 0.5-2.0 min; 60-10% Solvent A and 2.0-2.5 min; and 10% Solvent A. The separated sample was placed into the MS/MS part API5000™ (AB SCIEX, Framingham, Massachusetts, USA) equipped with Turbo Ion Spray as an ion source. Dipyridamole and ketoconazole were monitored by multiple reaction monitoring of the transitions of m/z 429.3 → 506.3 and m/z 531.4 → 82.1, respectively.

3.2.14. Statistical analysis

The data were statistically evaluated using the t-test. The results were considered significant at the 5% significance level ($p < 0.05$).

3.3. Results

3.3.1. Docking and binding affinity of L-PGDS for dipyridamole

The binding of dipyridamole molecule with the hydrophobic cavity of L-PGDS was

virtually observed by docking simulation program (Fig. 20A). The fluorescence quenching of the intrinsic tryptophan residue of L-PGDS was measured with the various concentration of dipyridamole to check the binding affinity of L-PGDS for dipyridamole. The concentration-dependent fluorescence quenching by the addition of dipyridamole was observed (Fig. 20B and C), and the calculated K_d value was 550 nM.

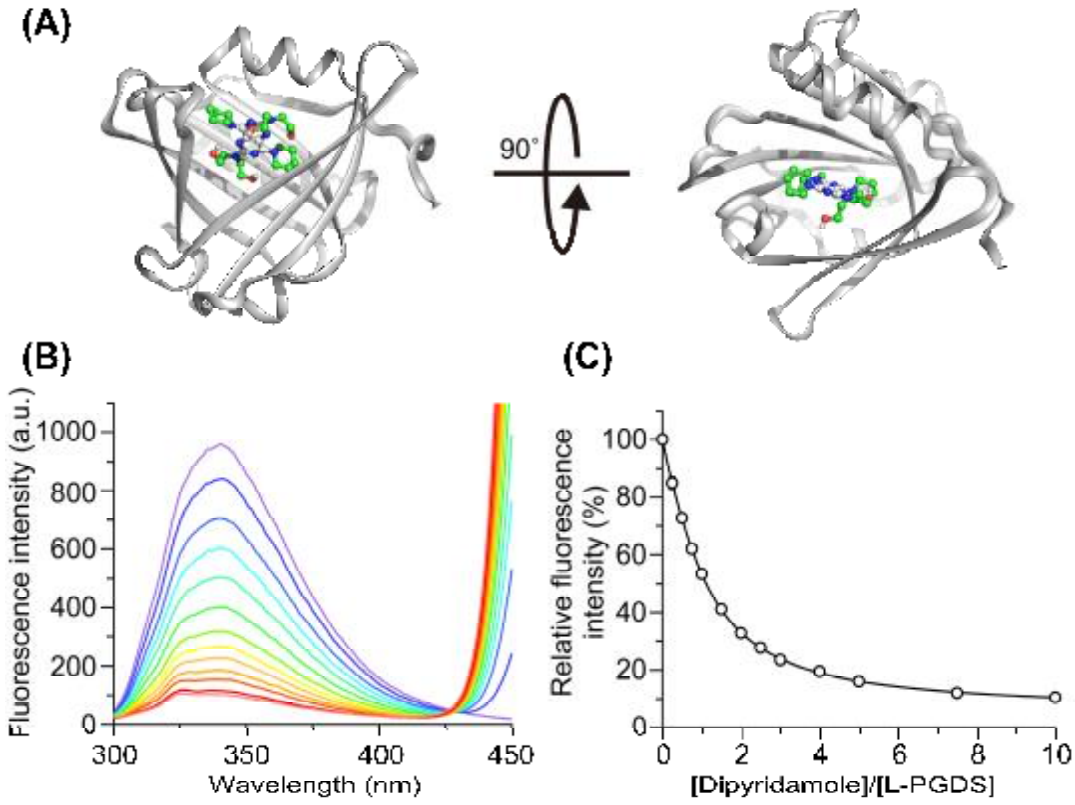

Figure 20 The binding affinity of L-PGDS for dipyridamole. (A) Structural model of dipyridamole/L-PGDS complex obtained by AutoDock Vina; (B) The emission spectrum of L-PGDS recorded at different concentrations of dipyridamole with excitation at 340 nm; and (C) The relative fluorescence intensity of L-PGDS.

3.3.2. Evaluation of solubility enhancement by L-PGDS

The solubility enhancement of dipyridamole was evaluated by the addition of L-PGDS in several kinds of buffer medium (Table 6). The preparation of the complex at 37°C for 2 h was sufficient to achieve equilibrium solubility in the preliminary evaluation. The solubility of dipyridamole (4.9-9.1 μg/mL) was significantly enhanced, approximately by 50-90 folds (425-440 μg/mL) with 25 mg of L-PGDS in all the evaluated mediums. There was no influence of buffer species, ion strength or physiological surface-active ingredients (taurocholate and lecithin) on the solubility enhancement of L-PGDS. In addition, a linear increase in dipyridamole solubility was observed by increasing the amount of L-PGDS in 5 mM Tris-HCl buffer of pH 8.0 (Table 7).

Table 6 Solubility of dipyridamole in the presence or absence of L-PGDS at 37°C in different pH buffers.

Medium	25 mg L-PGDS	μg/mL
FaSSGF (pH 1.6)	−	>100
FaSSIF (pH 6.5)	−	9.1
	+	440
50 mM Phosphate buffer (pH 6.8)	−	6.3
	+	431
5 mM Tris-HCl buffer (pH 8.0)	−	4.9
	+	425

FaSSGF, fasted state-simulated gastric fluid; FaSSIF, fasted state-simulated intestinal fluid
L-PGDS, lipocalin-type prostaglandin D synthase

Table 7 Solubility profile of dipyridamole with several concentrations of L-PGDS in 5 mM Tris-HCl buffer (pH 8.0).

	Solubility (μM)		
L-PGDS	0	270	1,330
Dipyridamole	10	202	842

L-PGDS, lipocalin-type prostaglandin D synthase

3.3.3. Physical characterization of spray-dried dipyridamole/L-PGDS complex

3.3.3.1. Spray-drying process of dipyridamole/L-PGDS complex solution

All spray-drying runs showed a high yield of 80-90% without any process issues. Only a small amount of powdery deposit was observed, and the inside wall of the drying chamber was cleaned.

3.3.3.2. Morphological analyses

The surface morphology of the spray-dried dipyridamole/L-PGDS complex powder was observed with SEM (Fig. 21). Dipyridamole was an agglutinate mixture of rectangular particles (Fig. 21A). The spray-dried dipyridamole/L-PGDS complex had typical spherical particles produced by spray drying (Fig. 21B).

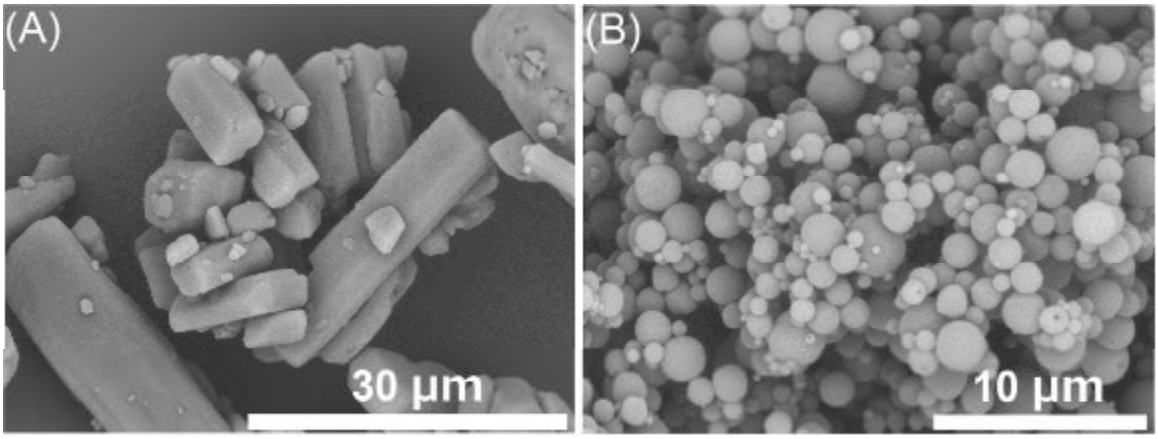

Figure 21 SEM images of (A) dipyridamole and (B) spray-dried dipyridamole/L-PGDS complex powder.

3.3.3.3. Hygroscopic profile

The hygroscopicity of the spray-dried powders was evaluated by water sorption/desorption isotherm measurement at 40°C (Fig. 22). There was no hysteresis gap

between the sorption and desorption phases, and it showed a reversible moisture uptake property. The produced powder absorbed about 20% water by increasing of the RH to 75%.

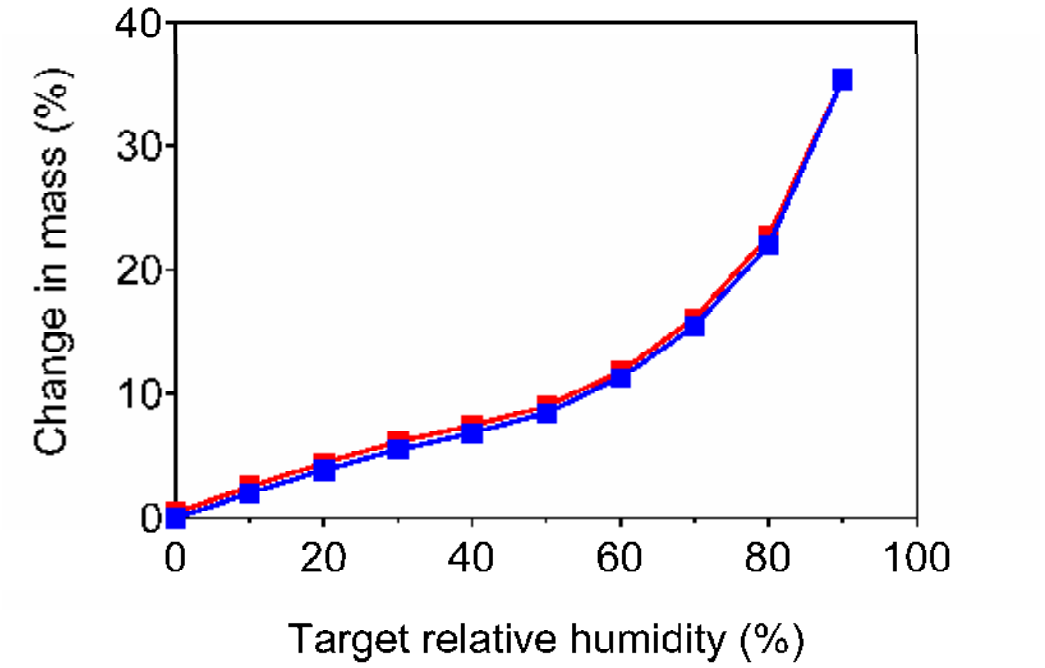

Figure 22 Water vapor isotherm plot of the spray-dried dipyridamole/L-PGDS complex at 40°C. Sorption (blue) and desorption (red).

3.3.3.4. Dissolution behavior

Small-scale dissolution testing was performed to evaluate the *in vitro* dissolution behavior of the spray-dried dipyridamole/L-PGDS complex in FaSSGF and phosphate buffer, pH 6.8 (Fig. 23). Dipyridamole was measured as a control of the dipyridamole/L-PGDS complex formulation. The dissolution level of dipyridamole in FaSSGF (pH 1.6) was 100% of the applied total amount of the drug (Fig. 23A), while the solubility in phosphate buffer at pH 6.8 was approximately 20% at 60 min (Fig. 23B). In contrast, the complex formulation of dipyridamole/L-PGDS significantly enhanced the solubility of

dipyridamole, and achieved approximately 100% dissolution within 5 min in both FaSSGF and phosphate buffer at pH 6.8 (Fig. 23A and 23B).

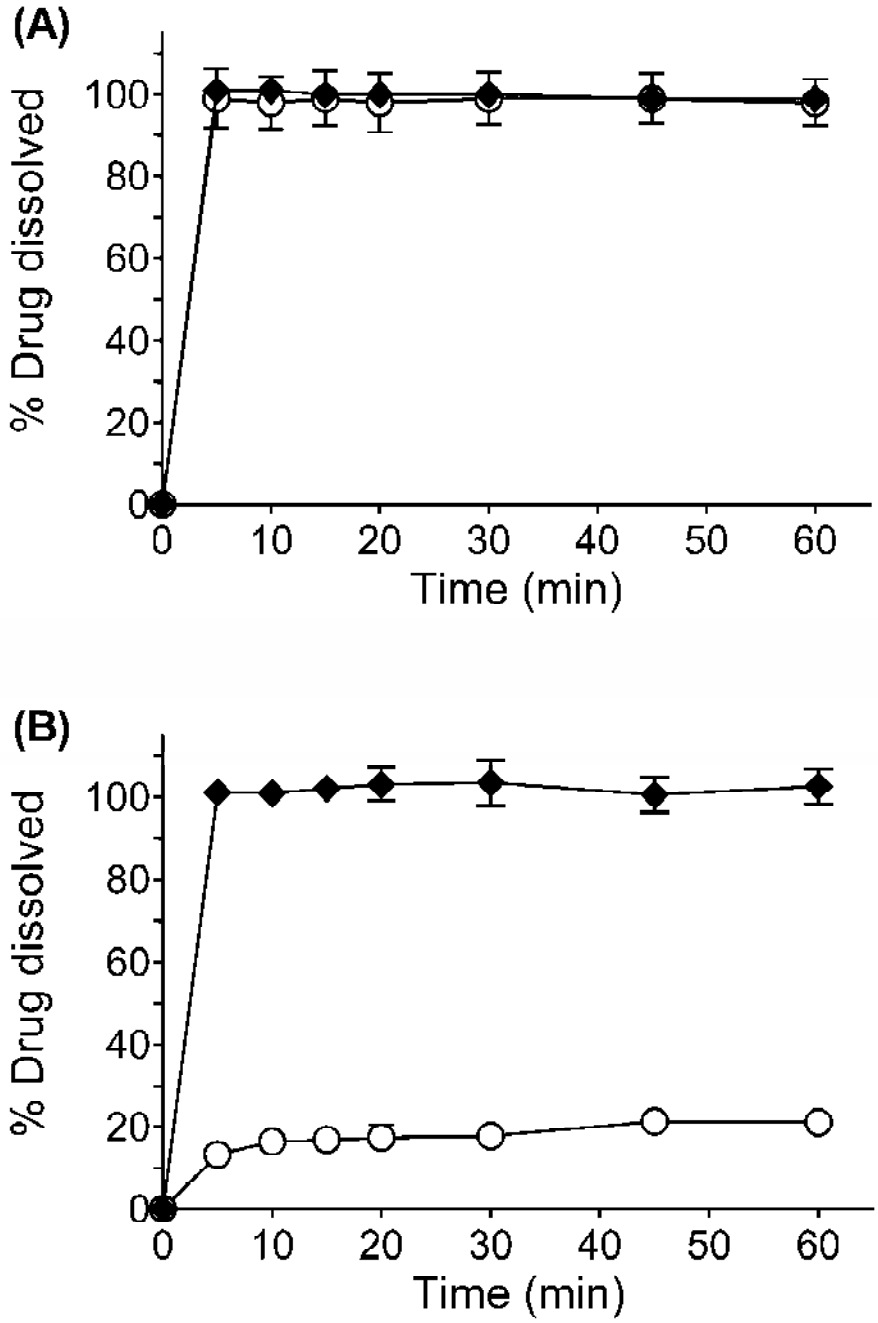

Figure 23 Dissolution profiles of dipyridamole formulations in (A) FaSSGF with pepsin (pH 1.6), and (B) phosphate buffer (pH 6.8). ○: dipyridamole and ¿: spray-dried dipyridamole/L-PGDS complex. Target concentration of dipyridamole: 0.05 mg/mL. Each bar represents the mean ± SD of three independent experiments.

3.3.4. Pharmacokinetic evaluation of solubilized formulation of dipyridamole with L-PGDS complex

The concentration of dipyridamole in plasma was measured to compare the *in vivo* behavior of the orally administered dipyridamole/L-PGDS complex in the normal rats and omeprazole pre-treated hypochlorhydria model rats (Fig. 24). The calculated pharmacokinetic parameters are summarized in Table 8. In normal rats, the dipyridamole and complex formulation showed comparable pharmacokinetic profiles. However, in the hypochlorhydria model rats, the $AUC_{0\text{-}24h}$ and C_{max} of dipyridamole formulation were markedly reduced in comparison with the normal rats (Fig. 24A and Table 8). In contrast, the pharmacokinetic behavior of the complex formulation was similar to that of the dipyridamole in the case of hypochlorhydria model rats (Fig. 24B). There was no significant difference in the T_{max} and $T_{1/2}$ in any of the evaluated formulations in the normal and hypochlorhydria model rats.

Table 8 Pharmacokinetic parameters of dipyridamole formulations after oral administration.

	Dipyridamole		*Dipyridamole/L-PGDS complex*	
	Normal rats	Hypochlorhydria model rats	Normal rats	Hypochlorhydria model rats
$AUC_{0\text{-}24h}$ (ng h/mL)	360.5 ± 40.6*	164.9 ± 16.4	363.6 ± 38.7*	386.5 ± 28.5*
C_{max} (ng/mL)	106.0 ± 32.4	65.1 ± 7.3	112.1 ± 29.8	119.6 ± 38.1
T_{max} (h)	0.4	0.3	0.3	0.3
$T_{1/2}$ (h)	2.5 ± 0.7	1.8 ± 0.7	2.0 ± 0.2	1.7 ± 0.4

L-PGDS, lipocalin-type prostaglandin D synthase

*: Significant difference from dipyridamole administered in hypochlorhydria model rats ($P < 0.05$)

Values ($AUC_{0\text{-}24h}$, C_{max}) are expressed as the mean ± S.E. of four experiments.

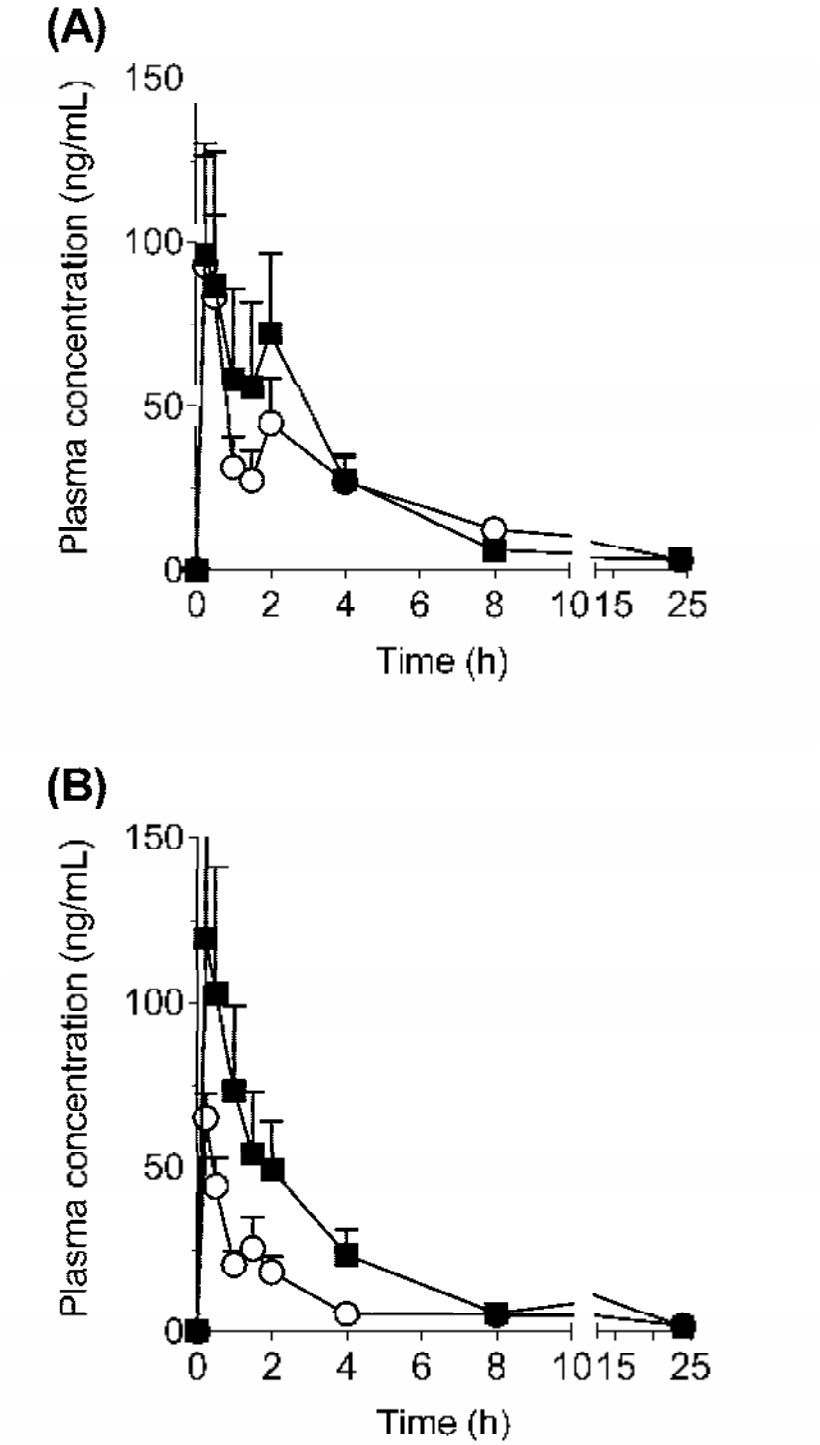

Figure 24 The time-profile of the plasma concentration of dipyridamole after oral administration in (A) normal rats and (B) omeprazole pre-treated hypo-chlorhydria model rats (7.5 mg/kg dipyridamole). ○: dipyridamole, **n**: dipyridamole/L-PGDS complex. Each bar represents the mean ± S.E. of four independent experiments.

3.4. Discussion

In this study, L-PGDS achieved the solubilization of dipyridamole, a weak basic compound, by forming a complex in the simple preparation process in the physiological pH range (Tables 6 and 7). Furthermore, the binding of dipyridamole into the hydrophobic cavity of L-PGDS was demonstrated virtually by the docking simulation (Fig. 20A), and the binding between dipyridamole and L-PGDS was considered to have higher affinity (K_d = 550 nM). Although L-PGDS has a limited ability to form a complex with a guest compound due to the size of the L-PGDS cavity, the capability of the currently developing low-molecular-weight drug candidates may be sufficient.

Dipyridamole is categorized as BCS class II compound. BCS, and the basic compound with pK_a of 6.4 showed poor solubility in buffer medium at or above a neutral pH (4.9-6.3 μg/mL, Table 6), whereas the compound is readily soluble in buffer medium at an acidic pH. Therefore, sufficient gastric acidity is a prerequisite for adequate dissolution and absorption. In the pharmacokinetic study using normal rats, there was no significant difference in pharmacokinetic behavior between dipyridamole and dipyridamole/L-PGDS complex formulation (Table 8). The high solubility of dipyridamole in the gastric juice at low pH is directly involved in the similar pharmacokinetic behaviors between dipyridamole and its complex formulation in the case of normal rats. This result was consistent with the high solubility of dipyridamole and its complex formulation in FaSSGF (pH 1.6) *in vitro* (Fig. 23A). In contrast, the absorption of dipyridamole in the omeprazole pre-treated hypochlorhydria model rats was markedly suppressed to ca. 45% of $AUC_{0\text{-}24h}$ and 60% of C_{max} compared to the results obtained in case of normal rats (Table 8). The pH of the gastric compartment was elevated up to 7.0 by pre-treatment with omeprazole, and an intragastric pH of more than 6.0 was maintained for

6 h [72]. Hence, the dissolved amount of dipyridamole in the gastric compartment of hypochlorhydria model rats would be lower than that of the normal rats, and the reduction in the amount of dissolved dipyridamole could suppress the absorption of dipyridamole in the hypochlorhydria model rats. On the other hand, the pharmacokinetic behavior of the complex formulation was similar to that of dipyridamole in the hypochlorhydria model rats (Table 8).

The driving force responsible for complex formulation between the L-PGDS and guest compound was found to be both hydrophilic and hydrophobic interactions adjusted by enthalpy-entropy compensation [21]. In addition, I have suggested that the drug release from the complex formulation is due to the degradation of L-PGDS with digestive enzymes, such as trypsin and chymotrypsin in the intestinal compartment, and not with pepsin in the stomach, which is based on the result obtained in chapter 2. Therefore, the change of the gastric pH would have no influence on drug release from the complex formulation.

The spray-drying process of the dipyridamole/L-PGDS complex solution was successfully performed and a high-yield process was achieved. The produced spray-dried dipyridamole/L-PGDS complex powder showed typical morphological properties (Fig. 21). No solid agglomerate was observed in the obtained powder. Hence, it was considered that the dipyridamole/L-PGDS complex solution was well dispersed without additives, such as surfactants and carbohydrates, to prevent agglomeration [73].

The small-scale dissolution test showed that the spray-dried dipyridamole/L-PGDS powder was dissolved immediately in both FaSSGF (pH 1.6) and phosphate buffer (pH 6.8) (Fig. 23). According to the Noyes–Whitney equation, the increase in the surface area due to the reduction in the particle size increased the dissolution rate [74]. Although

the particle size of dipyridamole was coarser than that of dipyridamole/L-PGDS powder judging from SEM images (Fig. 21), the dissolution profile in FaSSGF (pH 1.6) was comparable (Fig. 23A). It was considered that similar dissolution rate of dipyridamole and the complex formulation in FaSSGF could be caused by the fast intrinsic dissolution rate at a low pH [75].

The present study demonstrated that L-PGDS improved the absorption behavior of dipyridamole by the formation of a complex. This novel approach to developing a pH-independent formulation using L-PGDS is considered to overcome the clinical disadvantage of the weak basic drug in the elevated gastric pH environment.

3.5. Conclusions

The solubilization of dipyridamole was achieved by a simple complex formulation method involving L-PGDS. The complex formulation could overcome the problematic pH-dependent solubility profile of dipyridamole and solid state of the complex formulation was produced successfully by the spray-drying process. Furthermore, the dipyridamole/L-PGDS complex formulation improved the pharmacokinetic behavior of dipyridamole as observed in the hypochlorhydria model rats. This study demonstrated that L-PGDS is a well-designed carrier that effectively delivers the drug to the absorption site.

4

Assessment of the stability profile of spray-dried L-PGDS complex formulation

4.1. Introduction

The prepared L-PGDS/drug complex formulation was spray-dried in this work and the process produced drug/L-PGDS complex formulation without any issue, such as low yield, aggregation, and denaturation of L-PGDS. However, the spray-dried protein formulation has the possibility to observe the unfolding, aggregation and inactivation of protein during the storage [37, 42]. The inherent stability profile in the solid state of L-PGDS is still unknown. Furthermore, the change of interaction between L-PGDS and guest compounds in the solid state storage needs to be assessed. In this chapter, the stability study of spray-dried L-PGDS complex was performed to assess the potential stability profile of spray-dried L-PGDS complex formulation. This complex formulation was evaluated as the complex model formulation. The sample was stored in the several storage conditions up to three months, and the content of dipyridamole, secondary and tertiary structure of L-PGDS, aggregation, and dissolution profile of stored sample were evaluated.

4.2. Materials and methods

4.2.1. Purification of recombinant human L-PGDS

The isolation and purification process of recombinant human C65A/C167A (ε_{280} =25,900 M^{-1} cm^{-1})-substituted L-PGDS mutant was same as described in section 2.2.2 in chapter 2.

4.2.2. Spray drying of dipyridamole/L-PGDS complex solution

The preparation method for dipyridamole/L-PGDS complex formulation and process parameters for spray drying were same as described in section 3.2.6 in chapter 3. The produced powders were collected through a high-efficiency cyclone in a glass container, and stored at −20°C until the initiation of stability study.

4.2.3. Assay for dipyridamole content in complex formulation

The produced spray-dried powder of 2 mg was reconstituted in 100 μL of water, followed by addition of 900 μL of methanol for protein precipitation. After centrifugation at 15,000 rpm for 5 min, the supernatant was injected into the HPLC and analyzed according to the HPLC conditions as described in section 3.2.5.

4.2.4. CD measurement

The measurement condition was same as described in section 2.2.8 of chapter 2.

4.2.5. SE-HPLC

The analytical condition of SE-HPLC was same as described in section 2.2.7 in chapter 2.

4.2.6. Small-scale dissolution testing

The dissolution testing of the spray-dried dipyridamole/L-PGDS complex in 0.05 M phosphate buffer at pH 6.8 was implemented for 60 min at 37°C according to the test condition as described in section 3.2.12 of chapter 3.

4.2.7. Stability study

The samples were used to fill glass bottles, and were sealed with plastic caps and stored at 5°C in a temperature-controlled refrigerator, or 25°C/60% RH in a stability chamber SRH-32VEVJ2 (Nagano Science Co. Ltd., Osaka, Japan), or 40°C/75% RH in SRH-15VEVJ2 (Nagano Science Co. Ltd.) for closed storage. For open storage at 40°C/75% RH, the glass sample bottles without caps were stored in a stability chamber SRH-15VEVJ2 (Nagano Science Co. Ltd.). After one month (except for 5°C storage) and three months of storage, content of dipyridamole in the powder, the CD spectrum, content of soluble aggregates, and dissolution profile in phosphate buffer at pH 6.8 of the stored samples were evaluated according to the method as described in sections 4.2.3, 4.2.4, 4.2.5, and 4.2.6, respectively.

4.3. Results

4.3.1. Structure change evaluation of spray-dried dipyridamole/L-PGDS formulation

The structural change of the produced dipyridamole/L-PGDS complex formulation for temperature and humidity were assessed. The stored samples were reconstituted with 5 mM Tris-HCl (pH 8.0), and the CD spectrum of reconstituted samples was monitored to evaluate the changes of secondary and tertiary structures of the dissolved dipyridamole/L-PGDS complex. The samples stored under all storage conditions had the same CD spectrum as the initial ones in the far- and near-UV regions, respectively (Fig. 25 and 26).

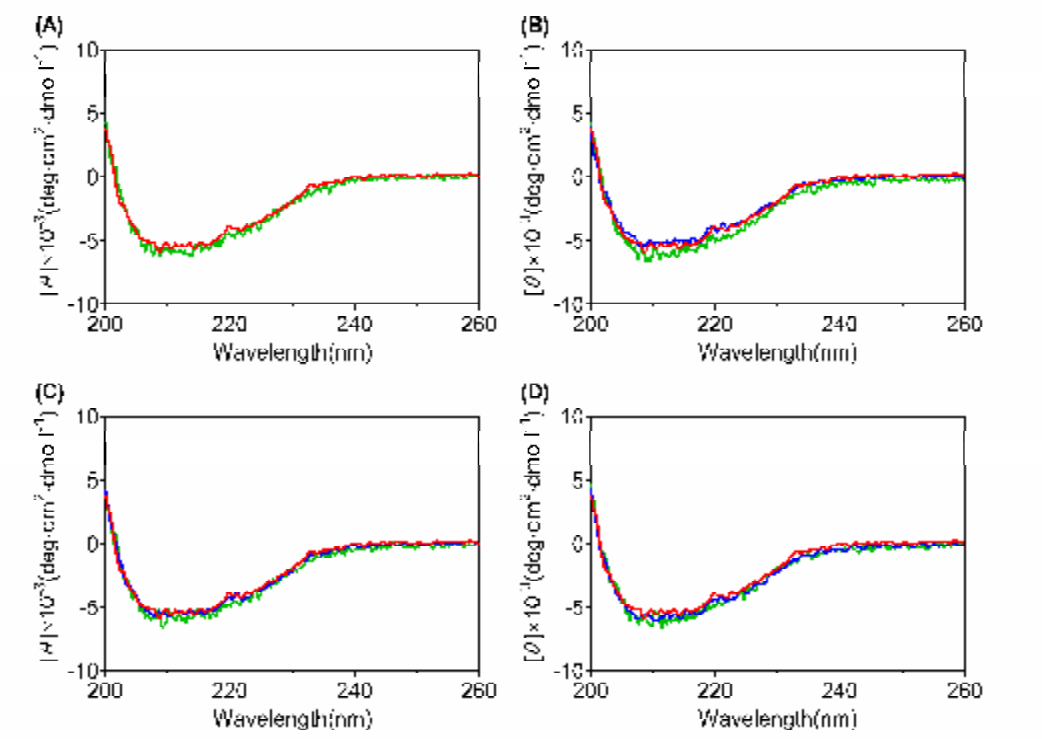

Figure 25 CD spectra in far-UV region of reconstituted initial complex formulation (red), reconstituted one month storage sample stored (blue) and reconstituted three months storage sample (green). (A): 5°C, (B): 25°C/60% RH, (C): 40°C/75% RH, and (D): 40°C/75% RH (open).

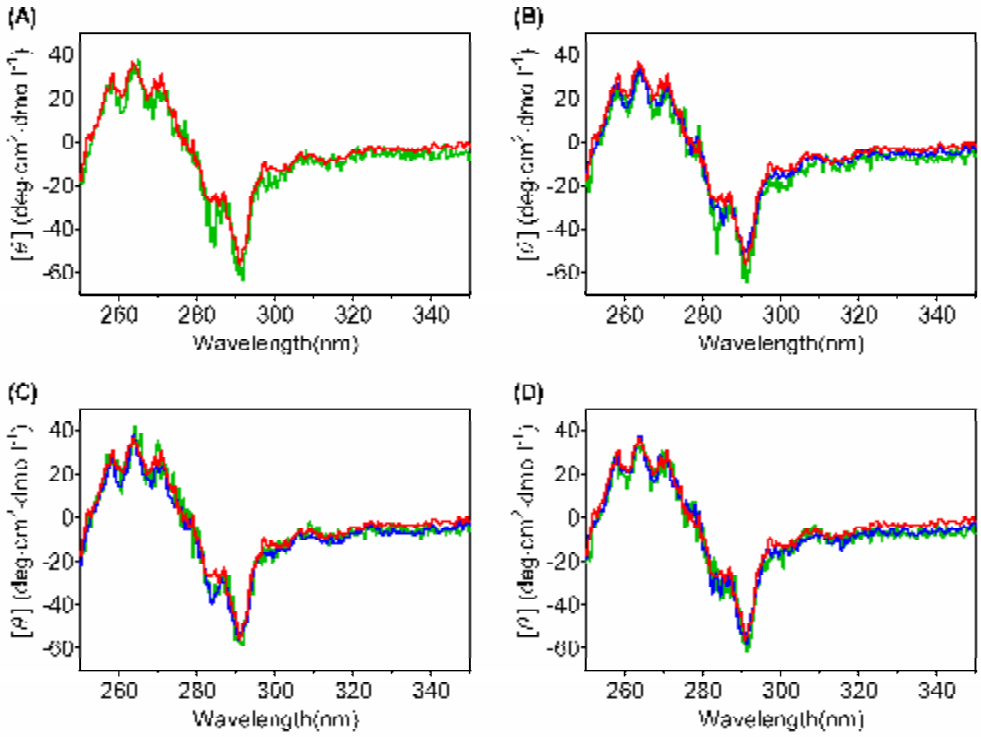

Figure 26 CD spectra in near-UV region of reconstituted initial complex formulation (red), reconstituted one month storage sample stored (blue) and reconstituted three months storage sample (green). (A): 5°C, (B): 25°C/60% RH, (C): 40°C/75% RH, and (D): 40°C/75% RH (open).

4.3.2. Evaluation of dipyridamole contents and soluble aggregation of L-PGDS

In addition, the dipyridamole content and soluble aggregation of the stored complex powder was analyzed and compared with the initial sample (Table 9). The samples that were stored at 5°C and 25°C/60% RH maintained the content of dipyridamole while a slight decrease of dipyridamole was observed in the sample stored at 40°C/75% RH and 40°C/75% RH (open). At one month storage, there was no soluble aggregation in the sample at 25°C/65% RH, but the samples at 40°C/75% RH and 40°C/75% RH (open) generated 1.4 and 5.2% soluble aggregates, respectively (Table 9). In addition, sample

at 25°C/60% RH generated 0.6% soluble aggregates. The amount of soluble aggregates in the samples at 40°C/75% RH and 40°C/75% RH (open) was found to increase at three months storage (Table 9).

Table 9 Dipyridamole content of the stored samples under each storage condition.

Storage condition	Storage period	Comparison with initial sample (%)	Soluble aggregate (%)
Initial	–	–	not detected
5°C	Three months	97.1 ± 8.58	not detected
25°C/60% RH	One month	100.1 ± 3.83	not detected
	Three months	98.4 ± 1.62	0.58 ± 0.01
40°C/75% RH	One month	96.4 ± 1.64	1.41 ± 0.01
	Three months	94.1 ± 3.91	4.14 ± 0.06
40°C/75% RH (open)	One month	93.4 ± 2.17	5.21 ± 0.02
	Three months	95.2 ± 2.47	10.46 ± 0.24

Values are presented as the mean ± SD of three experiments.

4.3.3. Dissolution profiles of stored dipyridamole/L-PGDS complex

Furthermore, the dissolution behavior of stored samples at pH 6.8 was checked (Fig. 27), and the powder stored at 5°C and 25°C/60% RH showed dissolution profiles comparable with the initial ones up to three months storage. On the other hand, the samples stored at 40°C/75% RH and 40°C/75% RH (open) slightly reduced the plateau level of dipyridamole dissolution. The reduced degree in the samples at 40°C/75% RH and 40°C/75% RH (open) had similarity with the result of changes in the dipyridamole content in the complex formulation (Table 6 and Fig. 24). In addition, an insoluble aggregation was observed in the reconstituted sample stored at 40°C/75% RH (open) for one and three months by visual inspection, and insoluble aggregation was shown by the sample at 40°C/75% RH for three-month storage.

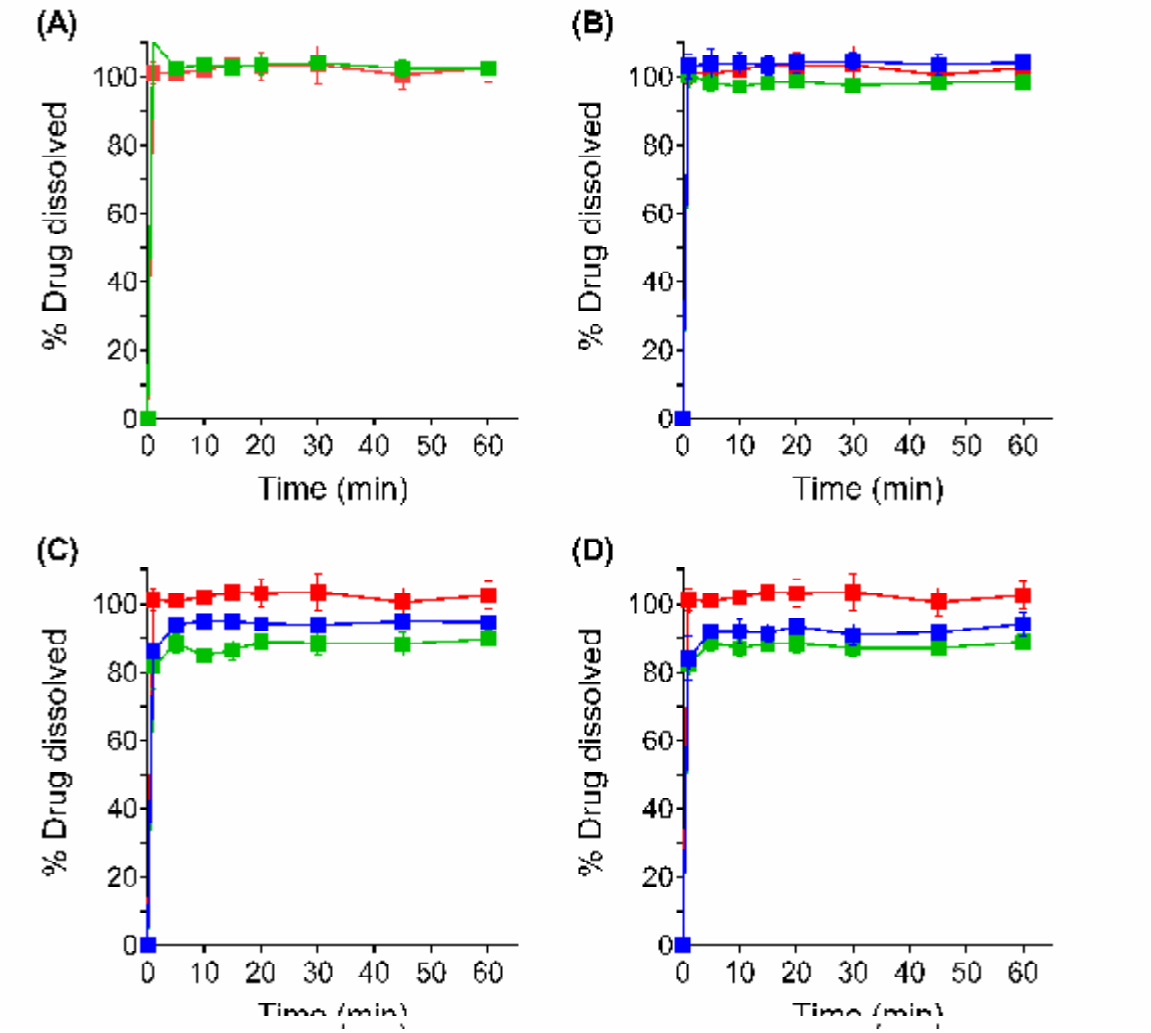

Figure 27 Dissolution profile at pH 6.8 of reconstituted initial complex formulation (red), reconstituted one month storage sample stored (blue), and reconstituted three months storage sample (green). (A): 5°C, (B): 25°C/60% RH, (C): 40°C/75% RH, and (D): 40°C/75% RH (open).

4.4. Discussion

The potential stability assessment for the spray-dried dipyridamole/L-PGDS was explored under the variable storage conditions. CD measurement showed no significant difference in the secondary or tertiary structures of the stored complex formulation (Fig. 25 and 26). Also, 4.1 and 10.5% of the soluble aggregates were detected under 40°C/75% RH and 40°C/75% RH (open) three months storage, respectively, but it was not detected at 5°C for three months. The samples at 25°C/60% RH for three months included 0.6% soluble aggregates. In addition, the insoluble aggregation was observed in the sample at 40°C/75% RH for three months and 40°C/75% RH (open) storage samples.

The produced dipyridamole/L-PGDS complex powder was composed of fine particles with a large specific surface area (Fig. 21B), and approximately 20% moisture gain at 40°C/75% RH was observed on DVS measurement (Fig. 22). Therefore, it was considered that the simple formulation of the dipyridamole/L-PGDS complex without any excipients might be sensitive to temperature and humidity. It has been demonstrated that the excipients like sugars and polyols improve the stability of dried-protein and formulations, such as antibody by the dilution of protein in the surface of solid particles and reduction of inter-molecular interactions during long-term storage [59, 76]. A further exploratory stability study of the complex should be conducted to evaluate the effect of suggested stabilizers of dried-protein formulations, such as sucrose and trehalose, on the quality of spray-dried L-PGDS for bulk storage.

Furthermore, the content of dipyridamole in the complex formulation was found to decrease slightly under 40°C/75% RH and 40°C/75% RH (open) storage (Table 9). Due to the weak susceptibility of dipyridamole to hydrolysis and oxidation [77], the reduction of the dipyridamole content and lower plateau level on dissolution testing of the com-

plex formulation with L-PGDS could be caused by the enhanced hydrolysis or oxidation of free dipyridamole (Table 9 and Fig. 27). The dissolution study of the stored samples revealed that the conformation of the dipyridamole/L-PGDS complex was maintained after storage under the conditions set in this study, but the increased insoluble aggregates including dipyridamole decreased the plateau level in the samples at 40°C/75% RH and 40°C/75% (open). The dissolution rate of all stored samples was comparable to that of the initial sample (Fig. 27).

4.5. Conclusion

In this chapter, the stability profiles of spray-dried dipyridamole/L-PGDS complex formulation were assessed. The spray-dried L-PGDS maintained the secondary and tertiary structures and kept the conformation of the complex at evaluated storage conditions. However, the humidity conditions led to the increase in the soluble and insoluble aggregates. The compatibility assessment with several excipients that are known as stabilizers for protein formulation should be evaluated for further investigation.

5
Summary

The majority of the developing low molecular weight drug substances have poor solubility. The current employed target-based approach using combinatorial chemistry and high throughput screening is considered to be the main approach for drug discovery process in the future. Therefore, the improvement of solubility for poorly-water soluble drug substance also seems to be a continued challenge for the formulation scientists, and the breakthrough of its concern increases the development accuracy and wipes out the unexpected clinical disorder, such as highly variable efficacy.

In the present work, the feasibility of L-PGDS as the pharmaceutical novel solubilizer for oral formulation was closely evaluated. In chapter 2, L-PGDS improved the solubility of telmisartan that showed poor solubility in physiological pH condition by the complexation. The complexation was prepared with the simple and easy process. The improved solubility of telmisartan showed a linear increase with the increase in the amount of L-PGDS. The dried particle of the highly soluble complex that consists of telmisartan and L-PGDS was manufactured with a spray dryer. The obtained particle had superior properties (spherical shape, fine particle size, and narrow size distribution, fast *in vitro* dissolution behavior at pH 1.6, 5, and 6.8) and high yield (80-86%).

Furthermore, the pharmacokinetic study with SHR rats was implemented to evaluate the *in vivo* behavior of telmisartan/L-PGDS complex. The complex showed improved *in vivo* behavior than API and improved AUC and T_{max} of the marketed product that includes pH-modifier in the formulation. In addition, the pharmacodynamics study exhib-

ited that the orally administered telmisartan/L-PGDS complex led to a rapid decrease in the mean systolic blood pressure, and the antihypertensive effect was held for more than 48 hours.

In chapter 3, the poorly-water soluble basic compound dipyridamole possessing the pH-dependent solubility profile was used as the model drug, and pH-independent drug release formulation using L-PGDS was developed. The improvement of solubility was observed in the whole of the physiological pH range, and the spray-dried dipyridamole/L-PGDS particle showed fast and complete dissolution at pH 1.6 and 6.8.

In addition, a pharmacokinetic study using hypochlorhydria model rats was performed to verify the improvement of the intestinal absorption behavior, and eventually the complex formulation overcame the problematic absorption profile of dipyridamole in the elevated gastric pH conditions.

In Chapter 4, the potential stability profile of spray-dried drug substance/L-PGDS complex formulation was evaluated using spray-dried dipyridamole/L-PGDS as model formulation. In three month storage at several conditions (5°C, 25°C/60%RH, 40°C/75% RH, and 40°C/75%RH (open)), the secondary and tertiary structures of L-PGDS and complex conformation with dipyridamole was maintained. However, the soluble and insoluble aggregates that are commonly generated in the storage of solid state protein formulation were observed. The further stability assessment to evaluate the effect of stabilizers, such as polyols and surfactants, should be performed. The degradation of dipyridamole was also detected in the stability study. The degradation could be considered as self-degradation of free dipyridamole. However, along with the complexation efficiency, the compatibility profile of guest compounds with L-PGDS needs to be evaluated.

These results demonstrated the feasibility of L-PGDS as a solubilizer for a solid oral formulation. This novel potent solubilizer improved the solubility of poorly-water soluble compounds with the simple and easy process, with the well-designed mechanism of drug release by the biodegradation of L-PGDS. It is considered that L-PGDS can enter one of the solutions for the solubility improvement of a poorly-soluble drug candidate.

References

[1] C.A. Lipinski, Drug-like properties and the causes of poor solubility and poor permeability, J Pharmacol Toxicol Methods, 44 (2000) 235-249.

[2] C.A. Lipinski, F. Lombardo, B.W. Dominy, P.J. Feeney, Experimental and computational approaches to estimate solubility and permeability in drug discovery and development settings, Adv Drug Deliv Rev, 46 (2001) 3-26.

[3] G.L. Amidon, H. Lennernas, V.P. Shah, J.R. Crison, A theoretical basis for a biopharmaceutic drug classification: the correlation of in vitro drug product dissolution and in vivo bioavailability, Pharm Res, 12 (1995) 413-420.

[4] M.S. Ku, W. Dulin, A biopharmaceutical classification-based Right-First-Time formulation approach to reduce human pharmacokinetic variability and project cycle time from First-In-Human to clinical Proof-Of-Concept, Pharm Dev Technol, 17 (2012) 285-302.

[5] Y. Kawabata, K. Wada, M. Nakatani, S. Yamada, S. Onoue, Formulation design for poorly water-soluble drugs based on biopharmaceutics classification system: basic approaches and practical applications, Int J Pharm, 420 (2011) 1-10.

[6] A. Fahr, X. Liu, Drug delivery strategies for poorly water-soluble drugs, Expert Opin Drug Deliv, 4 (2007) 403-416.

[7] R.L. Carrier, L.A. Miller, I. Ahmed, The utility of cyclodextrins for enhancing oral bioavailability, J Control Release, 123 (2007) 78-99.

[8] T. Loftsson, S.B. Vogensen, M.E. Brewster, F. Konradsdottir, Effects of cyclodextrins on drug delivery through biological membranes, J Pharm Sci, 96 (2007) 2532-2546.

[9] V.M. Rao, V.J. Stella, When can cyclodextrins be considered for solubilization purposes?, J Pharm Sci, 92 (2003) 927-932.

[10] J.B. Zawilska, J. Wojcieszak, A.B. Olejniczak, Prodrugs: a challenge for the drug development, Pharmacol Rep, 65 (2013) 1-14.

[11] R.G. Strickley, Solubilizing excipients in oral and injectable formulations, Pharm Res, 21 (2004) 201-230.

[12] A. Fukuhara, M. Yamada, K. Fujimori, Y. Miyamoto, T. Kusumoto, H. Nakajima,

T. Inui, Lipocalin-type prostaglandin D synthase protects against oxidative stress-induced neuronal cell death, Biochem J, 443 (2012) 75-84.
[13] A. Nagata, Y. Suzuki, M. Igarashi, N. Eguchi, H. Toh, Y. Urade, O. Hayaishi, Human brain prostaglandin D synthase has been evolutionarily differentiated from lipophilic-ligand carrier proteins, Proc Natl Acad Sci U S A, 88 (1991) 4020-4024.
[14] H. Toh, H. Kubodera, N. Nakajima, T. Sekiya, N. Eguchi, T. Tanaka, Y. Urade, O. Hayaishi, Glutathione-independent prostaglandin D synthase as a lead molecule for designing new functional proteins, Protein Eng, 9 (1996) 1067-1082.
[15] T. Inui, M. Mase, R. Shirota, M. Nagashima, T. Okada, Y. Urade, Lipocalin-type prostaglandin D synthase scavenges biliverdin in the cerebrospinal fluid of patients with aneurysmal subarachnoid hemorrhage, J Cereb Blood Flow Metab, 34 (2014) 1558-1567.
[16] Y. Miyamoto, S. Nishimura, K. Inoue, S. Shimamoto, T. Yoshida, A. Fukuhara, M. Yamada, Y. Urade, N. Yagi, T. Ohkubo, T. Inui, Structural analysis of lipocalin-type prostaglandin D synthase complexed with biliverdin by small-angle X-ray scattering and multi-dimensional NMR, J Struct Biol, 169 (2010) 209-218.
[17] S. Shimamoto, T. Yoshida, T. Inui, K. Gohda, Y. Kobayashi, K. Fujimori, T. Tsurumura, K. Aritake, Y. Urade, T. Ohkubo, NMR solution structure of lipocalin-type prostaglandin D synthase: evidence for partial overlapping of catalytic pocket and retinoic acid-binding pocket within the central cavity, J Biol Chem, 282 (2007) 31373-31379.
[18] Y. Zhou, N. Shaw, Y. Li, Y. Zhao, R. Zhang, Z.J. Liu, Structure-function analysis of human l-prostaglandin D synthase bound with fatty acid molecules, FASEB J, 24 (2010) 4668-4677.
[19] T. Inui, T. Ohkubo, M. Emi, D. Irikura, O. Hayaishi, Y. Urade, Characterization of the unfolding process of lipocalin-type prostaglandin D synthase, J Biol Chem, 278 (2003) 2845-2852.
[20] S. Kume, Y.H. Lee, Y. Miyamoto, H. Fukada, Y. Goto, T. Inui, Systematic interaction analysis of human lipocalin-type prostaglandin D synthase with small lipophilic ligands, Biochem J, 446 (2012) 279-289.
[21] S. Kume, Y.H. Lee, M. Nakatsuji, Y. Teraoka, K. Yamaguchi, Y. Goto, T. Inui, Fine-tuned broad binding capability of human lipocalin-type prostaglandin D synthase

for various small lipophilic ligands, FEBS Lett, 588 (2014) 962-969.
[22] A. Fukuhara, H. Nakajima, Y. Miyamoto, K. Inoue, S. Kume, Y.H. Lee, M. Noda, S. Uchiyama, S. Shimamoto, S. Nishimura, T. Ohkubo, Y. Goto, T. Takeuchi, T. Inui, Drug delivery system for poorly water-soluble compounds using lipocalin-type prostaglandin D synthase, J Control Release, 159 (2012) 143-150.
[23] A. Kumari, S.K. Yadav, S.C. Yadav, Biodegradable polymeric nanoparticles based drug delivery systems, Colloids Surf B Biointerfaces, 75 (2010) 1-18.
[24] M. Vert, J. Mauduit, S. Li, Biodegradation of PLA/GA polymers: increasing complexity, Biomaterials, 15 (1994) 1209-1213.
[25] F. Danhier, O. Feron, V. Preat, To exploit the tumor microenvironment: Passive and active tumor targeting of nanocarriers for anti-cancer drug delivery, J Control Release, 148 (2010) 135-146.
[26] M. Wang, M. Thanou, Targeting nanoparticles to cancer, Pharmacol Res, 62 (2010) 90-99.
[27] P. Vishnu, V. Roy, Safety and Efficacy of nab-Paclitaxel in the Treatment of Patients with Breast Cancer, Breast Cancer (Auckl), 5 (2011) 53-65.
[28] V.P. Torchilin, Recent advances with liposomes as pharmaceutical carriers, Nat Rev Drug Discov, 4 (2005) 145-160.
[29] K. Tahara, T. Sakai, H. Yamamoto, H. Takeuchi, N. Hirashima, Y. Kawashima, Improved cellular uptake of chitosan-modified PLGA nanospheres by A549 cells, Int J Pharm, 382 (2009) 198-204.
[30] G.M. Subramanian, M. Fiscella, A. Lamouse-Smith, S. Zeuzem, J.G. McHutchison, Albinterferon alpha-2b: a genetic fusion protein for the treatment of chronic hepatitis C, Nat Biotechnol, 25 (2007) 1411-1419.
[31] A. Prokop, J.M. Davidson, Nanovehicular Intracellular Delivery Systems, J Pharm Sci, 97 (2008) 3518-3590.
[32] O. Pillai, R. Panchagnula, Polymers in drug delivery, Curr Opin Chem Biol, 5 (2001) 447-451.
[33] D.E. Owens, 3rd, N.A. Peppas, Opsonization, biodistribution, and pharmacokinetics of polymeric nanoparticles, Int J Pharm, 307 (2006) 93-102.
[34] D. Litvak-Greenfeld, I. Benhar, Risks and untoward toxicities of antibody-based immunoconjugates, Adv Drug Deliv Rev, 64 (2012) 1782-1799.

[35] F. Kratz, B. Elsadek, Clinical impact of serum proteins on drug delivery, J Control Release, 161 (2012) 429-445.
[36] F. Kratz, Albumin as a drug carrier: design of prodrugs, drug conjugates and nanoparticles, J Control Release, 132 (2008) 171-183.
[37] A.M. Abdul-Fattah, D.S. Kalonia, M.J. Pikal, The challenge of drying method selection for protein pharmaceuticals: product quality implications, J Pharm Sci, 96 (2007) 1886-1916.
[38] W. Wang, Lyophilization and development of solid protein pharmaceuticals, Int J Pharm, 203 (2000) 1-60.
[39] W. Wang, Instability, stabilization, and formulation of liquid protein pharmaceuticals, Int J Pharm, 185 (1999) 129-188.
[40] H.C. Mahler, R. Muller, W. Friess, A. Delille, S. Matheus, Induction and analysis of aggregates in a liquid IgG1-antibody formulation, Eur J Pharm Biopharm, 59 (2005) 407-417.
[41] K. Cal, K. Sollohub, Spray drying technique. I: Hardware and process parameters, J Pharm Sci, 99 (2010) 575-586.
[42] G. Lee, Spray-Drying of Proteins, in: J. Carpenter, M. Manning (Eds.) Rational Design of Stable Protein Formulations, Springer US, 2002, pp. 135-158.
[43] W. Wienen, M. Entzeroth, J.C.A. van Meel, J. Stangier, U. Busch, T. Ebner, J. Schmid, H. Lehmann, K. Matzek, J. Kempthorne-Rawson, V. Gladigau, N.H. Hauel, A Review on Telmisartan: A Novel, Long-Acting Angiotensin II-Receptor Antagonist, Cardiovascular Drug Reviews, 18 (2000) 127-154.
[44] P.H. Tran, H.T. Tran, B.J. Lee, Modulation of microenvironmental pH and crystallinity of ionizable telmisartan using alkalizers in solid dispersions for controlled release, J Control Release, 129 (2008) 59-65.
[45] M. Nakatani, Takeshi, S., Ohki, T., Toyoshima, SOLID PHARMACEUTICAL FORMULATIONS COMPRISING TELMISARTAN, in: U. ptent (Ed.), 2004.
[46] C. Taniguchi, Y. Kawabata, K. Wada, S. Yamada, S. Onoue, Microenvironmental pH-modification to improve dissolution behavior and oral absorption for drugs with pH-dependent solubility, Expert Opin Drug Deliv, 11 (2014) 505-516.
[47] S.I. Badawy, M.A. Hussain, Microenvironmental pH modulation in solid dosage forms, J Pharm Sci, 96 (2007) 948-959.

[48] L. Zhong, X. Zhu, X. Luo, W. Su, Dissolution properties and physical characterization of telmisartan-chitosan solid dispersions prepared by mechanochemical activation, AAPS PharmSciTech, 14 (2013) 541-550.
[49] M. Sangwai, P. Vavia, Amorphous ternary cyclodextrin nanocomposites of telmisartan for oral drug delivery: improved solubility and reduced pharmacokinetic variability, Int J Pharm, 453 (2013) 423-432.
[50] N. Marasini, T.H. Tran, B.K. Poudel, H.J. Cho, Y.K. Choi, S.C. Chi, H.G. Choi, C.S. Yong, J.O. Kim, Fabrication and evaluation of pH-modulated solid dispersion for telmisartan by spray-drying technique, Int J Pharm, 441 (2013) 424-432.
[51] M. Vertzoni, J. Dressman, J. Butler, J. Hempenstall, C. Reppas, Simulation of fasting gastric conditions and its importance for the in vivo dissolution of lipophilic compounds, Eur J Pharm Biopharm, 60 (2005) 413-417.
[52] E. Galia, E. Nicolaides, D. Horter, R. Lobenberg, C. Reppas, J.B. Dressman, Evaluation of various dissolution media for predicting in vivo performance of class I and II drugs, Pharm Res, 15 (1998) 698-705.
[53] S. Reagan-Shaw, M. Nihal, N. Ahmad, Dose translation from animal to human studies revisited, FASEB J, 22 (2008) 659-661.
[54] M. Morihara, N. Aoyagi, N. Kaniwa, S. Kojima, H. Ogata, Assessment of gastric acidity of Japanese subjects over the last 15 years, Biol Pharm Bull, 24 (2001) 313-315.
[55] R.H. Hunt, D. Armstrong, C. James, S.K. Chowdhury, Y. Yuan, P. Fiorentini, A. Taccoen, P. Cohen, Effect on intragastric pH of a PPI with a prolonged plasma half-life: comparison between tenatoprazole and esomeprazole on the duration of acid suppression in healthy male volunteers, Am J Gastroenterol, 100 (2005) 1949-1956.
[56] W.N. Charman, C.J. Porter, S. Mithani, J.B. Dressman, Physiochemical and physiological mechanisms for the effects of food on drug absorption: the role of lipids and pH, J Pharm Sci, 86 (1997) 269-282.
[57] R. Vehring, Pharmaceutical particle engineering via spray drying, Pharm Res, 25 (2008) 999-1022.
[58] S.A. Shoyele, N. Sivadas, S.A. Cryan, The effects of excipients and particle engineering on the biophysical stability and aerosol performance of parathyroid hormone (1-34) prepared as a dry powder for inhalation, AAPS PharmSciTech, 12 (2011) 304-311.

[59] S. Schule, T. Schulz-Fademrecht, P. Garidel, K. Bechtold-Peters, W. Frieb, Stabilization of IgG1 in spray-dried powders for inhalation, Eur J Pharm Biopharm, 69 (2008) 793-807.
[60] W.L. Hulse, R.T. Forbes, M.C. Bonner, M. Getrost, Influence of protein on mannitol polymorphic form produced during co-spray drying, Int J Pharm, 382 (2009) 67-72.
[61] W. Wienen, H.J. Schierok, Effects of telmisartan, hydrochlorothiazide and their combination on blood pressure and renal excretory parameters in spontaneously hypertensive rats, J Renin Angiotensin Aldosterone Syst, 2 (2001) 123-128.
[62] K. Sugano, Computational oral absorption simulation of free base drugs, Int J Pharm, 398 (2010) 73-82.
[63] T.L. Russell, R.R. Berardi, J.L. Barnett, L.C. Dermentzoglou, K.M. Jarvenpaa, S.P. Schmaltz, J.B. Dressman, Upper gastrointestinal pH in seventy-nine healthy, elderly, North American men and women, Pharm Res, 10 (1993) 187-196.
[64] E. Lahner, B. Annibale, G. Delle Fave, Systematic review: Helicobacter pylori infection and impaired drug absorption, Aliment Pharmacol Ther, 29 (2009) 379-386.
[65] C. Patrono, B. Coller, J.E. Dalen, G.A. FitzGerald, V. Fuster, M. Gent, J. Hirsh, G. Roth, Platelet-active drugs : the relationships among dose, effectiveness, and side effects, Chest, 119 (2001) 39S-63S.
[66] S.C. Rabbie, T. Flanagan, P.D. Martin, A.W. Basit, Inter-subject variability in intestinal drug solubility, Int J Pharm, 485 (2015) 229-234.
[67] H. Derendorf, C.P. VanderMaelen, R.S. Brickl, T.R. MacGregor, W. Eisert, Dipyridamole bioavailability in subjects with reduced gastric acidity, J Clin Pharmacol, 45 (2005) 845-850.
[68] V.M. Rao, E.A. Zannou, V.J. Stella, Design of tablets for the delayed and complete release of poorly water-soluble weak base drugs using SBE7M-beta-CD as a solubilizing agent, J Pharm Sci, 100 (2011) 1576-1587.
[69] J.E. Patterson, M.B. James, A.H. Forster, R.W. Lancaster, J.M. Butler, T. Rades, Preparation of glass solutions of three poorly water soluble drugs by spray drying, melt extrusion and ball milling, Int J Pharm, 336 (2007) 22-34.
[70] S. Onoue, R. Inoue, C. Taniguchi, Y. Kawabata, K. Yamashita, K. Wada, Y. Yamauchi, S. Yamada, Improved dissolution and pharmacokinetic behavior of

dipyridamole formulation with microenvironmental pH-modifier under hypochlorhydria, Int J Pharm, 426 (2012) 61-66.
[71] F. Guo, H. Zhong, J. He, B. Xie, F. Liu, H. Xu, M. Liu, C. Xu, Self-microemulsifying drug delivery system for improved oral bioavailability of dipyridamole: preparation and evaluation, Arch Pharm Res, 34 (2011) 1113-1123.
[72] I. Wada, M. Otaka, M. Jin, M. Odashima, K. Komatsu, N. Konishi, T. Matsuhashi, Y. Horikawa, R. Ohba, H. Itoh, S. Watanabe, Expression of HSP72 in the gastric mucosa is regulated by gastric acid in rats-correlation of HSP72 expression with mucosal protection, Biochem Biophys Res Commun, 349 (2006) 611-618.
[73] A. Millqvist-Fureby, M. Malmsten, B. Bergenstahl, Spray-drying of trypsin - surface characterisation and activity preservation, Int J Pharm, 188 (1999) 243-253.
[74] S.B. Murdande, D.A. Shah, R.H. Dave, Impact of nanosizing on solubility and dissolution rate of poorly soluble pharmaceuticals, J Pharm Sci, 104 (2015) 2094-2102.
[75] C. Taniguchi, R. Inoue, Y. Kawabata, K. Yamashita, K. Wada, Y. Yamauchi, S. Yamada, S. Onoue, Novel formulations of dipyridamole with microenvironmental pH-modifiers for improved dissolution and bioavailability under hypochlorhydria, Int J Pharm, 434 (2012) 148-154.
[76] W.J. Fang, W. Qi, J. Kinzell, S. Prestrelski, J.F. Carpenter, Effects of excipients on the chemical and physical stability of glucagon during freeze-drying and storage in dried formulations, Pharm Res, 29 (2012) 3278-3291.
[77] B.K. Vaghela, S.S. Rao, P.S. Reddy, Development and validation of a stability indicating RP-LC method for the estimation of process related impurities and degradation products of dipyridamole retard capsules, Int J Pharm Pharm Sci, 4, Suppl 1 (2012) 615-622.

Appendix

Parts of this work have been published to the following journals.

Masashi Mizoguchi, Masatoshi Nakatsuji, Haruka Inoue, Keisuke Yamaguchi, Atsushi Sakamoto, Koichi Wada, Takashi Inui,

Novel oral formulation approach for poorly water-soluble drug using lipocalin-type prostaglandin D synthase.

Eur. J. Pharm. Sci., **74**, 77-85, 2015.

Masashi Mizoguchi, Masatoshi Nakatsuji, Junichi Takano, Osamu Ishibashi, Koichi Wada, Takashi Inui,

Development of pH-independent drug release formulation using lipocalin-type prostaglandin D synthase

J. Pharm. Sci., **in press** (accepted on 24th Nov., 2015)

Acknowledgement

I would like to take the opportunity to thank all of people who supported me through the course towards the completion of my PhD.

Foremost, I would like to thank my advisor Prof. Dr. Takashi Inui for providing the opportunity for PhD work on this objective. He always advised me and his guidance helped me in all the time of research, publication of scientific articles and writing this thesis. His suggestion helped me greatly in bringing out the best result in this work.

I am extremely grateful to Dr. Koichi Wada, Dr. Chika Taniguchi and Dr. Roman Messerschmid for the approval and support to perform my PhD at the department of CMC, KPRI, Nippon Boehringer Ingelheim Co., Ltd.

I would like to thank the members of Laboratory of Biological Macromolecules, especially Mr. Masatoshi Nakatsuji and Mr. Keisuke Yamaguchi to supports in the several experiments for my PhD. Moreover, I would like to thank the colleagues of Nippon Boehringer Ingelheim Co., Ltd, especially Dr. Atsushi Sakamoto and Mr. Junichi Takano to support my experiments kindly. My research would not have been possible without their helps.

Finally, I express my heartfelt gratitude to my family for their support and patience. And I would like to thank my wife, Yoshimi for her support and encouragement. Also, I would also like to thank my parents, and elder sister. They were always encouraging me with their best wishes.

Masashi Mizoguchi

2016